

AD-A107 480

HARRY DIAMOND LABS ADELPHI MD

F/G 16/4.2

SCALE MODELING FOR THE PATRIOT ELECTROMAGNETIC PULSE TEST.(U)

MAY 81 A A CUNEO, J J LOFTUS

UNCLASSIFIED

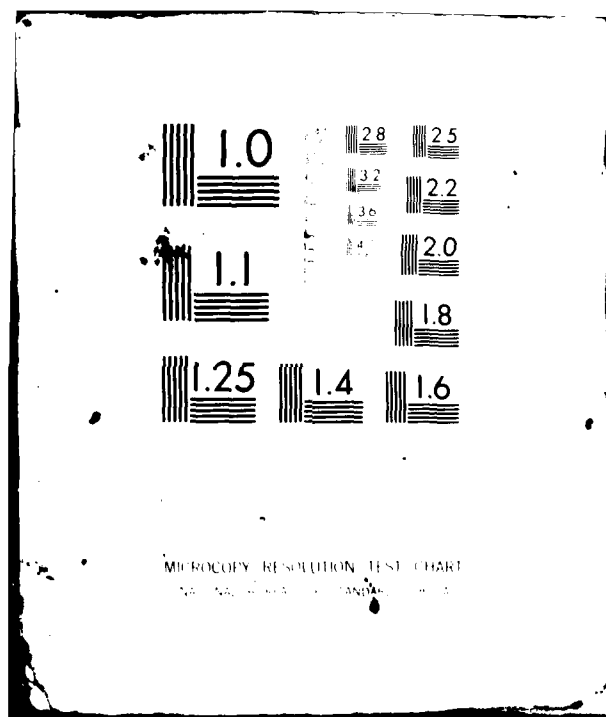
HDL-TM-81-16

NL

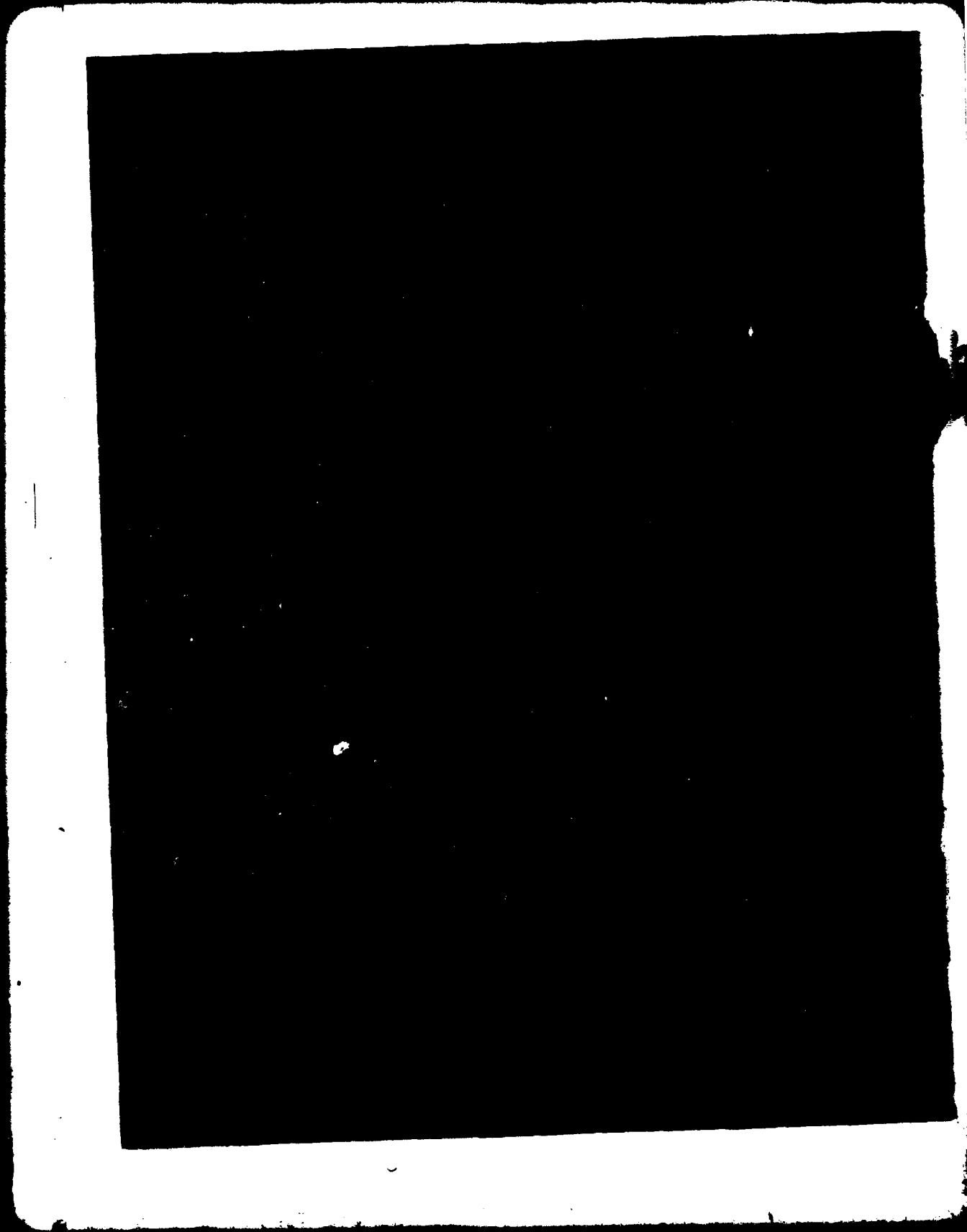
1 2

40 7810





AD A107480



UNCLASSIFIED

SECURITY CLASSIFICATION OF THIS PAGE (When Data Entered)

REPORT DOCUMENTATION PAGE		READ INSTRUCTIONS BEFORE COMPLETING FORM
1. REPORT NUMBER HDL-TM-81-16	2. GOVT ACCESSION NO. AD-A107480	3. RECIPIENT'S CATALOG NUMBER
4. TITLE (and Subtitle) Scale Modeling for the PATRIOT Electromagnetic Pulse Test.		5. TYPE OF REPORT & PERIOD COVERED Technical Memorandum
7. AUTHOR(s) Andrew A. Cuneo, Jr. James J. Loftus		6. PERFORMING ORG. REPORT NUMBER
9. PERFORMING ORGANIZATION NAME AND ADDRESS Harry Diamond Laboratories 2800 Powder Mill Road Adelphi, MD 20783		8. CONTRACT OR GRANT NUMBER(s)
11. CONTROLLING OFFICE NAME AND ADDRESS Project Manager PATRIOT Missile System, USADARCOM Redstone Arsenal, AL 35809		10. PROGRAM ELEMENT, PROJECT, TASK AREA & WORK UNIT NUMBERS Program Ele: 6.43.07.A
14. MONITORING AGENCY NAME & ADDRESS (if different from Controlling Office)		12. REPORT DATE May 1981
		13. NUMBER OF PAGES 100
		15. SECURITY CLASS. (of this report) UNCLASSIFIED
		15a. DECLASSIFICATION/DOWNGRADING SCHEDULE
16. DISTRIBUTION STATEMENT (of this Report) Approved for public release; distribution unlimited.		
17. DISTRIBUTION STATEMENT (of the abstract entered in Block 20, if different from Report)		
18. SUPPLEMENTARY NOTES DRCMS Code: 644307.21.20012 DA Project: 1X464307D212 HDL Project: E449E4		
19. KEY WORDS (Continue on reverse side if necessary and identify by block number) EMP Scale modeling Coupling System		
20. ABSTRACT (Continue on reverse side if necessary and identify by block number) The Harry Diamond Laboratories performed experimental electromagnetic coupling studies of a scale model of the PATRIOT air defense system as part of the evaluation of this system's ability to survive exposure to an electromagnetic pulse (EMP). This exercise was primarily concerned with providing basic information that is either too costly and time consuming or impossible to obtain in a full-scale field operation. This		

DD FORM 1 JAN 73 1473 EDITION OF 1 NOV 65 IS OBSOLETE

1

UNCLASSIFIED

SECURITY CLASSIFICATION OF THIS PAGE (When Data Entered)

UNCLASSIFIED

SECURITY CLASSIFICATION OF THIS PAGE(When Data Entered)

20. ABSTRACT (Cont'd)

basic information consists of the answers to such questions as these: how the external receptor currents change with variations of the incident field's azimuthal and elevation angles as well as polarization, what the effect of cable routing is on EMP coupling, and how critical the system grounding is to EMP protection.

Accession For	
NTIS GRA&I	<input checked="checked" type="checkbox"/>
DTIC TAB	<input type="checkbox"/>
Unannounced	<input type="checkbox"/>
Justification	
By _____	
Distribution/	
Availability Codes	
Dist	Avail and/or Special
A	

UNCLASSIFIED

CONTENTS

	<u>Page</u>
1. INTRODUCTION	9
2. PATRIOT SYSTEM DESCRIPTION	9
3. MODELING	10
3.1 Theory	10
3.2 Scope and Application	11
3.3 Scale Modeling Facility	11
3.4 Instrumentation	12
3.4.1 Pulse Generator	12
3.4.2 Pulse Radiator, Horizontal	12
3.4.3 Pulse Radiator, Vertical	14
3.4.4 Measurement Equipment	14
3.5 Radiated Field Measurements	14
4. EXPERIMENTAL DATA	17
4.1 Approach	17
4.1.1 System Configuration 1	19
4.1.2 System Configuration 2	20
4.1.3 System Configuration 3	21
4.1.4 System Configuration 4	22
4.1.5 System Configuration 5	22
4.1.6 System Configuration 6	23
4.1.7 System Configuration 7	23
4.1.8 System Configuration 8	25
4.1.9 System Configuration 9	25
4.1.10 Measurement System Noise	26
4.2 Horizontal Polarization Data	26
4.3 Effects of Number of PATRIOT Vehicles	40
4.4 Effects of Vehicle Grounds	40
4.5 Effects of Cable Routing	44
4.6 Coupling to ECS to EPP Cable with and without AMG and AMG to ECS Cable	44
4.7 Angle of Incidence Variation	49
4.8 Current Sharing on Parallel Conductors Illuminated by Electromagnetic Wave	53
4.9 Vertical Polarization Data	54
4.10 Comparison of Horizontal and Vertical Data	54
5. SCALING UP DATA BY USING SCALING LAWS WITH ASSOCIATED PROBLEMS ..	66
5.1 General Considerations	66

CONTENTS (Cont'd)

	<u>Page</u>
5.2 Scaling Permittivity and Conductivity	66
5.3 Coupling to Cable on and Above Ground in Real World and Model	68
6. CONCLUSIONS	76
LITERATURE CITED	77
DISTRIBUTION	99

APPENDICES

A. CALCULATION OF FIELDS FROM VERTICALLY AND HORIZONTALLY POLARIZED RADIATORS FOR PATRIOT SYSTEM ILLUMINATION	79
B. EXPERIMENT OF PATRIOT SYSTEM TO STUDY COUPLING TO COLLINEARLY ARRANGED ENGAGEMENT CONTROL STATION, ANTENNA MAST GROUP, AND ELECTRIC POWER PLANT	83
C. EXPERIMENT OF PATRIOT SYSTEM TO COMPARE THE RESPONSE OF A MODEL WIRE ABOVEGROUND WITH HORIZONTALLY AND VERTICALLY POLARIZED INCIDENT FIELDS	89
D. RADIATED FIELD WAVEFORMS OF PATRIOT SYSTEM	95

FIGURES

1 PATRIOT fire control center	10
2 Scale modeling facility	12
3 Loaded dipole antenna illuminator	13
4 Computer integrated output of conical monopole field sensor	16
5 Computer integrated output of conical dipole sensor with sensor calibration factor included	17
6 Configuration 1	19
7 Configuration 2	20
8 Configuration 3	21
9 Configuration 4	22
10 Configuration 5	23
11 Configuration 6	24

FIGURES (Cont'd)

	<u>Page</u>
12 Configuration 7	24
13 Configuration 8	25
14 Configuration 9	26
15 Explanation of file name and example of data	27
16 Configuration 1 histogram for test point 1	28
17 Configuration 1 polar plot for test point 1	28
18 Configuration 1 histogram for test point 2	29
19 Configuration 1 polar plot for test point 2	30
20 Configuration 1 histogram for test point 3	30
21 Configuration 1 polar plot for test point 3	31
22 Superposition of configuration test points 1, 2, and 3 in histogram form	32
23 Superposition of configuration test points 1, 2, and 3 in polar form	32
24 Configuration 5: plan view	33
25 Configuration 7: plan view	33
26 Configuration 5 histogram for test point 1	34
27 Configuration 5 histogram for test point 2	34
28 Configuration 5 histogram for test point 3	35
29 Configuration 5 polar plot for test point 1	35
30 Configuration 5 polar plot for test point 2	36
31 Configuration 5 polar plot for test point 3	36
32 Configuration 7 histogram for test point 1	37
33 Configuration 7 histogram for test point 2	37
34 Configuration 7 histogram for test point 3	38
35 Configuration 7 polar plot for test point 1	38
36 Configuration 7 polar plot for test point 2	39
37 Configuration 7 polar plot for test point 3	39
38 Configuration 2, showing center of rotation	41
39 Configuration 2 histogram for test point 1	41
40 Configuration 2 polar plot for test point 1	42

FIGURES (Cont'd)

	<u>Page</u>
41 Configuration 6 histogram for test point 2	42
42 Configuration 6 polar plot for test point 2	43
43 Configuration 6 histogram for test point 3	43
44 Configuration 6 polar plot for test point 3	44
45 Effects of wire routing for configuration 6	45
46 Effects of wire routing for configuration 4	46
47 Effect of antenna mast group to engagement control station (ECS) wire on current on ECS to electric power plant wire	47
48 Test with antenna mast group to engagement control station wire for test point 1, three vehicles each grounded	48
49 Test with antenna mast group to engagement control station wire for test point 1, four vehicles each grounded and AMG attached ..	48
50 Test with antenna mast group to engagement control station cable for test point 1, four vehicles all grounded and mast removed from AMG	49
51 Waveforms of figures 48 and 49 superimposed	50
52 Fast Fourier transforms of figure 51 waveforms	50
53 Configurations: loop versus two vehicles	51
54 Loop versus two vehicles: 10-deg elevation angle	51
55 Loop versus two vehicles: 45-deg elevation angle	52
56 Loop versus two vehicles: 90-deg elevation angle	52
57 Comparison of loop fast Fourier transforms for 90- and 10-deg angles of elevation	53
58 Configuration 9 vertical polarization experiment, test point 1 three vehicles, no antenna mast group	55
59 Configuration 9 vertical polarization experiment, test point 1, antenna mast group attached but not grounded	56
60 Configuration 9 vertical polarization experiment, test point 1, antenna mast group attached and grounded	56
61 Configuration 9 vertical polarization experiment, test point 2, three vehicles, no antenna mast group	57
62 Configuration 9 vertical polarization experiment, test point 2, antenna mast group attached but not grounded	57

FIGURES (Cont'd)

	<u>Page</u>
63 Configuration 9 vertical polarization experiment, test point 2, antenna mast group attached and grounded	58
64 Configuration 9 vertical polarization experiment, test point 3, three vehicles, no antenna mast group	58
65 Configuration 9 vertical polarization experiment, test point 3, antenna mast group attached but not grounded	59
66 Configuration 9 vertical polarization experiment, test point 3, antenna mast group attached and grounded	59
67 Configuration 9 vertical polarization experiment, test point 1, three vehicles grounded, no antenna mast group	60
68 Configuration 9 vertical polarization experiment, test point 1, antenna mast group in place but not grounded	60
69 Configuration 9 vertical polarization experiment, test point 1, antenna mast group in place and grounded	61
70 Configuration 9 vertical polarization experiment, test point 2, three vehicles each grounded, no antenna mast group	61
71 Configuration 9 vertical polarization experiment, test point 2, antenna mast group in place but not grounded	62
72 Configuration 9 vertical polarization experiment, test point 2, antenna mast group in place and grounded	62
73 Configuration 9 vertical polarization experiment, test point 3, three vehicles each grounded, no antenna mast group	63
74 Configuration 9 vertical polarization experiment, test point 3, antenna mast group in place but not grounded	63
75 Configuration 9 vertical polarization experiment, test point 3, antenna mast group in place and grounded	64
76 Configuration 9 test point 1	65
77 Wire aboveground	69
78 Wire on ground	70
79 Horizontally polarized model incident field, magnetic field measurement	70

TABLES

1 Experimental Configurations	18
2 Results of System Configuration 8 Experiment	40

TABLES (Cont'd)

	<u>Page</u>
3 Configuration 3 and 4 Responses	47
4 Configuration 1 and 6 Responses	47
5 Current Sharing Experimental Data	54
6 Response of PATRIOT Model to Vertical Illumination	64
7 Dielectric Constant and Conductivity of REPS Soil (Surface)	67
8 Dielectric Constant and Conductivity of REPS Soil (6-in. Depth) .	67
9 Dielectric Constant and Conductivity of Model Soil	68
10 Actual Model Parameter Values and Scaled REPS Values	68
11 Peak to Peak Current on Wire in Model and in Front of REPS	69

1. INTRODUCTION

Electronic equipment is potentially vulnerable to the electromagnetic pulse (EMP) caused by the detonation of a nuclear weapon at high altitudes. Military electronic systems that are field deployed and composed of several units are particularly vulnerable. The command, control, communication, and primary power cables that link these units are excellent couplers for large amounts of energy from the incident field to the electronics.

The Harry Diamond Laboratories (HDL) performed experimental coupling studies of a scale model of the PATRIOT air defense system as part of the evaluation of this system's ability to survive exposure to EMP. This exercise was primarily concerned with providing basic data that are either too costly and time-consuming or impossible to obtain in a full-scale field operation.

Namely, how do the external receptor currents change with variation of the incident field's azimuthal and elevation angles as well as polarization? What is the effect of cable routing on EMP coupling? How critical is system grounding to EMP protection? The answers to these questions will be invaluable in deploying the PATRIOT for full-scale testing as well as for assessing the configuration that will best minimize the impact of an EMP threat.

2. PATRIOT SYSTEM DESCRIPTION

The PATRIOT is a mobile system designed to provide Army air defense using guided missiles. The system will detect, identify, track, and destroy high- or low-altitude targets.¹ The missiles are mounted on launching stations that are not physically connected to the fire control section (FCS). Fire control is maintained by a very high frequency (vhf) data radio link from the launch sites to the FCS.

The FCS is composed of four mobile units: the engagement control station (ECS), the antenna mast group (AMG), the radar set (RS), and an electric power plant (EPP). All of the FCS units are interconnected by cables that are potential EMP receptors (fig. 1).

The units that comprise the FCS were scale modeled to 1/50 of their actual size for this experimental coupling study.

¹PATRIOT Air Defense System, Raytheon Co. Missile Systems Div., PATRIOT Progr Office, Bedford, MA, Br. 10165, Rev. A (February 1978).

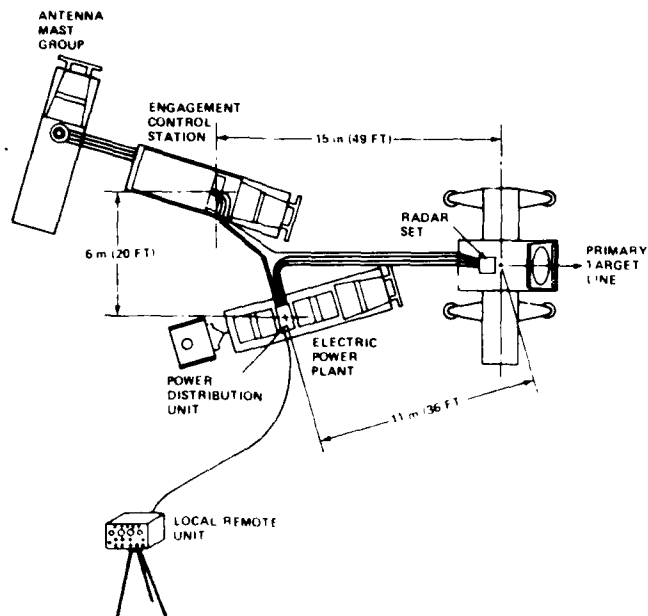


Figure 1. PATRIOT fire control center.

3. MODELING

3.1 Theory

The fact that electromagnetic scale modeling is possible in general is due to the linearity of Maxwell's equations that describe the fields in any electromagnetic system. It is necessary, therefore, to eliminate nonlinear media from the system of interest. In theory, it is not necessary to exclude nonhomogeneous media since Maxwell's equations are valid for nonhomogeneous as well as homogeneous media.

Sinclair shows that "for an arbitrary choice of the four scale factors p , α , β , and γ it is theoretically possible to construct an exact model to simulate a given full-scale system."² The scale factors are defined as follows:

- p = mechanical (linear dimension) scale factor,
- α = scale factor for electric field intensity,
- β = scale factor for magnetic field intensity,
- γ = scale factor for time.

²G. Sinclair, *Theory of Models of Electromagnetic Systems*, Proceedings of IRE (November 1948), 1364-1370.

Sinclair proceeds to show that when air in the full-scale system is simulated with air in the model, the following relationships are established for all media being modeled:

$$\begin{aligned}\mu' &= \mu \text{ (permeability),} \\ \epsilon' &= \epsilon \text{ (permittivity),} \\ \sigma' &= p\sigma \text{ (conductivity),} \\ p &= \gamma, \\ \alpha &= \beta,\end{aligned}$$

where the primed macroscopic properties refer to the model media and the unprimed properties refer to the full-scale system.

3.2 Scope and Application

The scope of this effort is to supply sufficient external receptor (cable) coupling information so that one can make intelligent decisions regarding the optimum layout of the PATRIOT system to minimize the impact of the EMP threat. The modeling also provides the kind of basic information needed to design the best possible type of test to determine the system's vulnerability.

For the PATRIOT model, $p = 50$, so that all physical dimensions have been scaled down by $1/50$. Copper was used to fabricate all shelters, trucks, and cables (wires were used to model cables) because copper affords the highest practical value of conductivity.

Previous tests at this facility have shown that the rise time of the currents induced in buried cables increases significantly as compared with the radiated-fielded rise time because of the high-frequency losses in the ground. These losses will increase the rise time also for cables lying on the ground as in the case of the PATRIOT. As will be seen, the rise time of the radiated field in the model was 200 ps.

3.3 Scale Modeling Facility

The HDL Electromagnetic Scale Modeling Facility occupies a large, essentially wooden structure at the North Annex of Fort Belvoir, VA. The structure, which is known as the Facility for Research in Electromagnetic Effects (FREME), is approximately 46×30 m, with the highest point of the roof 15 m above the floor (fig. 2).

The modeling is carried out in an 18×24 m box containing chemically treated sand of 10-cm average depth.

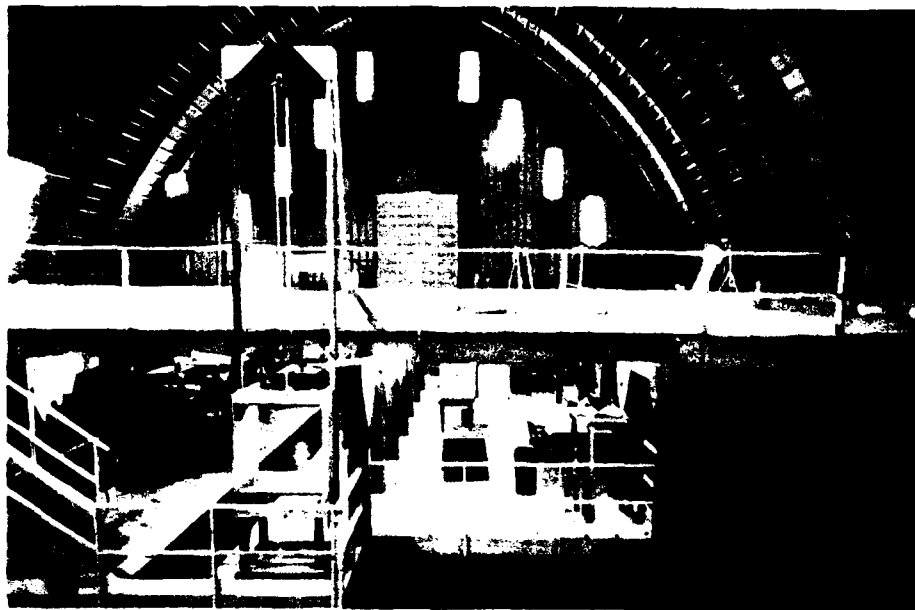


Figure 2. Scale modeling facility.

3.4 Instrumentation

3.4.1 Pulse Generator

The pulse generator used for this test was designed and built by HDL personnel. It consists of a coaxial-cable charge line of variable length attached to a commercial high-voltage direct current (dc) power supply. This discharges through the contacts of a mercury-wetted reed relay to the attached load. The mercury switch is housed in an aluminum casing that closely maintains a 50-ohm coaxial configuration from the charge line to the load. The aluminum allows the switch to be repetitively operated by the field induced from an alternating current (ac)-line-fed coil surrounding the casing. The output of this device is a variable-length pulse with a 150-ps rise time and a level of up to 1000 V into 50 ohms. The shape of the pulse is determined by a series capacitor inserted in the output. The output pulse is then coupled to the model antenna through a low-loss coaxial line.

3.4.2 Pulse Radiator, Horizontal

The output pulse of the generator was used to drive a horizontally polarized loaded dipole (LDP) antenna. The LDP antenna is a cylindrical dipole that is center fed by a bicone (fig. 3). This

bicone has a half angle of approximately 7 deg, yielding an impedance of 300 ohms, and a half length of 0.46 m, which is easily sufficient to launch the leading edge of the pulse without distortion. The bicone is joined to two 10-cm-diameter cylinders, which radiate the late time of the pulse. The overall length of the LDP is 6.6 m.

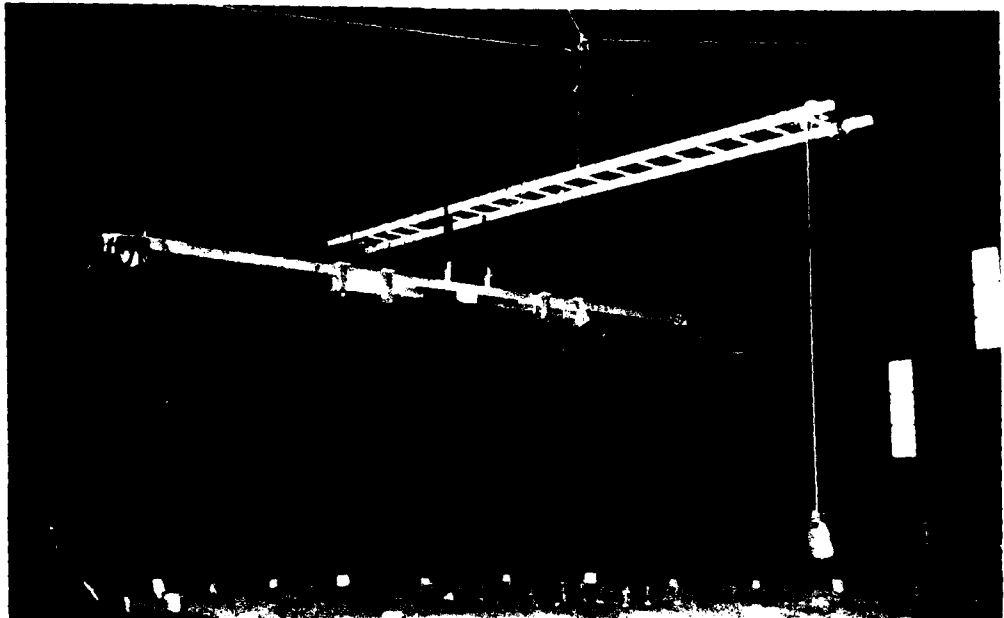


Figure 3. Loaded dipole antenna illuminator.

One side of the LDP is at dc ground and is used to house the radio frequency (rf) coaxial cable that conducts the remotely generated pulse to the bicone apex. The other side of the antenna is connected to the center conductor of the coaxial cable. End reflections are minimized by loading the ends of the antenna with rf-absorbent material.

The output of the generator was adjusted to yield an 860-V pulse applied to the LDP bicone, which, with an impedance-mismatch factor of 1.7, provided a bicone voltage of 1461 V. At a distance of 3.1 m, in the equatorial plane of the bicone, the calculated value of the free electric field is 94 V/m. The actual measurement of this field is discussed in section 3.5.

3.4.3 Pulse Radiator, Vertical

The vertical illumination of the PATRIOT was obtained by applying the pulse source to a resistively tapered monopole over a ground plane. The impedance of this monopole was determined to be 335 ohms by time domain reflectometry. This value yields an impedance-mismatch factor of 1.74, which would provide a monopole driving voltage of 1462 V. Using the 3-m distance yields a calculated value of 87 V/m for the free electric field. (See sect. 3.5 for comparison with measured field.)

3.4.4 Measurement Equipment

The HDL Electromagnetic Scale Modeling Facility uses time domain sampling (TDS) techniques to observe the responses of systems under test. This use is necessary since compliance with the scaling laws requires a radiated field with an extremely fast (≤ 250 ps) rise time, which precludes the use of real-time oscilloscopes. The use of TDS has recently been enhanced through the application of a digital processing oscilloscope (DPO) controlled by a minicomputer (Tektronix WP1221 Word Processing System). The computer allows one to signal average probe and sensor responses, which greatly enhance the signal to noise ratio. Of equal importance is the system's capability for mathematical manipulation of any collected waveform. This capability includes fast Fourier transforms (FFT's), inverse fast Fourier transforms (IFFT's), and integration, as well as others. Programs have been implemented in the computer that effectively compensate for the high-frequency losses of the rf cables and delay lines that are required to couple from the model the extremely fast rise time of the simulated EMP.

The measurement equipment and the computer are housed in a shielded enclosure.

3.5 Radiated Field Measurements

The rise time and the peak amplitude of the radiated field were measured for this test by using both a conical dipole (CD) field sensor and a conical monopole (CM) field sensor. These techniques are the latest efforts at this facility to increase the accuracy with which

extremely fast data (rise time of 250 ps) are obtained. The results of the horizontal³ and vertical field measurements will be published separately, and only a synopsis of the results is presented here.

A very small monopole sensor was fabricated at HDL and calibrated in a small transmission line. The output of the sensor is proportional to the derivative of the input. The output waveform is computer integrated, and the resulting waveform is stored on a magnetic disc. The applied voltage and the plate spacing of the transmission line being known, a calibration factor for the sensor was derived by assuming a transverse electromagnetic (TEM) mode of propagation since $E = V/h$, where E is the electric field, V is the voltage across the plates, and h is the plate spacing. This yielded a calibration factor of 8.3×10^{12} V/m/Vs, where Vs is the unit volts times seconds, which is the amplitude unit of an integrated time domain waveform.

The CM sensor was placed in the center of a 12-ft (3.7-m) square ground plane, made of brass screen and positioned 3 m from the resistively loaded vertical radiator. Figure 4 shows the computer integrated results of this measurement. The peak of the waveform when multiplied by the transmission line derived calibration factor yields

$$(1.19 \times 10^{-11} \text{ Vs})(8.3 \times 10^{12} \text{ V/m/Vs}) = 98.8 \text{ V/m} \quad .$$

This compares reasonably well with a calculated value of 87 V/m (app A). It is believed that the resistive loading of this vertical radiator causes the ringing seen on the waveform. The second peak (maximum of waveform) is caused by the first resistive load on the antenna. It can be seen, however, that the radiated field is rising very quickly and has reached 80 percent of peak value in only 203 ps. For a 1/50 scale model, this corresponds to a real rise time of 10.2 ns.

A second sensor was used to measure the horizontal field. This unit is a CD, which in effect is just two of the monopoles back to back and separated by a small common ground plate. This CD sensor was exposed to the field of the horizontal radiator mentioned previously at

³Andrew A. Cuneo, Jr., and James J. Loftus, *Measurement of Scaled Down High-Altitude Electromagnetic Pulse (HEMP) Waveforms*, Harry Diamond Laboratories HDL-TM-81-6) (March 1981).

a slant range of 3.1 m. The same high-frequency cable was used to carry the signal of both sides of the sensor to the recording instrumentation. While the response of one side of the CD sensor was sampled and stored on a magnetic disc, the other side was terminated in 50 ohms. This procedure was then reversed, with care taken so as not to disturb the physical positioning of the CD sensor relative to the radion source or the oscilloscope trigger source. Once both outputs had been recorded in this manner, it was a simple matter to reverse the polarity of the waveform representing the response of one side and add it to the other by using the computer. In this way, the common mode rejection characteristic of a balanced output sensor was maintained. Examination of this waveform shows a peak amplitude of 2.1×10^{-11} Vs.

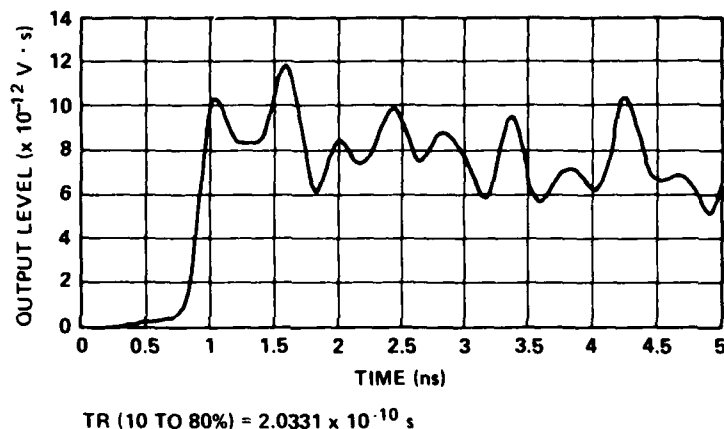


Figure 4. Computer integrated output of conical monopole field sensor (sensing vertical field).

This yields

$$(2.1 \times 10^{-11} \text{ Vs})(4.15 \times 10^{12} \text{ Vm/Vs}) = 87 \text{ V/m}$$

as shown in figure 5.

The CD sensor measured value of 87.0 V/m is within 8 percent of the calculated value of 94.0 V/m (app A).

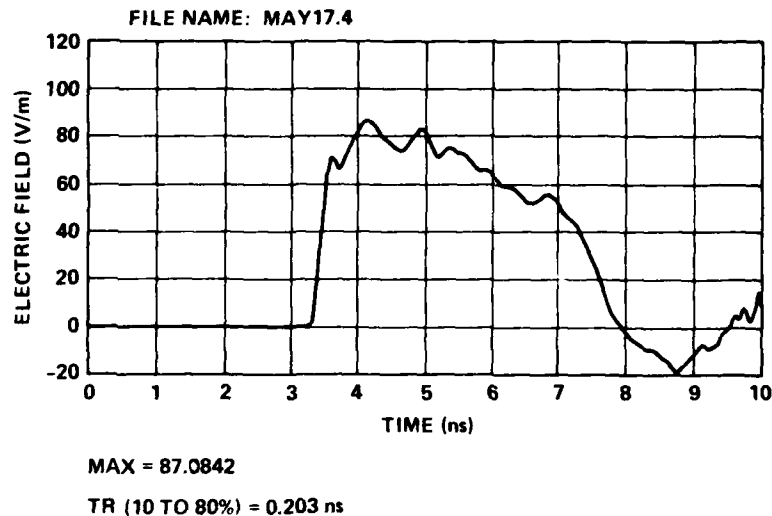


Figure 5. Computer integrated output of conical dipole sensor with sensor calibration factor included (sensing horizontal field).

4. EXPERIMENTAL DATA

4.1 Approach

The PATRIOT air defense system is presently scheduled to be exposed to EMP simulation at the HDL Woodbridge Research facility. Before an adequate test plan can be written, those responsible for the testing must decide how to deploy the PATRIOT with respect to the simulation source. That is, they must decide what angular relationship between the simulator and the PATRIOT represent the worst case for EMP coupling. One purpose of this scale-model experimental effort is to provide data that represent how the external receptors of the PATRIOT respond to the EMP when its azimuthal angle and elevation angle are varied. Further, data are provided to show how the system response will change with alteration of the PATRIOT system configuration. The model data were taken under the conditions summarized in table 1.

TABLE 1. EXPERIMENTAL CONFIGURATIONS

System Configuration	Polarization	Full 360-deg azimuth	Angle of incidence (deg)	Wire lengths (ft)	Ground	Wire spacing shape	Comments
1	Horizontal	Yes	45	1,1,2 ECS to RS = 2	All vehicles	Loose Y	--
2	Horizontal	Yes	45	2 ECS to RS	All vehicles	--	To observe response of single wire versus loop
3	Horizontal	No	45	2,2,2	All vehicles	~A	Maximum loop area of all configurations
4	Horizontal	No	45	3,2,2 ECS to RS = 3	All vehicles	Loose Y	--
5	Horizontal	Yes	45	3,2,2 ECS to RS = 3	Only on electric power plant	Tight Y	To observe effect of removing grounds
6	Horizontal	Yes	45	3,2,2 ECS to RS = 3	All vehicles	Tight Y	--
7	Horizontal	Yes	45	1,1,2 ECS to RS = 2	All vehicles	Loose Y	Same as configuration 1 except for local/remote unit wire
8	Horizontal	No	10,20 45,70	1,1,2 ECS to RS = 2	All vehicles	Loose Y	Add antenna mast group
9	Vertical	No	--	1,1,2 ECS to RS = 2	All vehicles	Loose Y	Add antenna mast group

Note: ECS = engagement control station; RS = radar set.

4.1.1 System Configuration 1

For configuration 1, the 1/50 model was deployed over the sand of the modeling facility as shown in figure 6. The model units were interconnected by nominally 0.050-in. (0.13-cm)-diameter (No. 16) enamel coated wire that lay on the sand. One-foot (0.3-m) wires, which were 50 ft (15 m) full scale, connected the EPP to the RS and to the ECS while a 2 ft (0.6-m) wire, which was 100 ft (30 m) full scale, was used between the ECS and the RS. Although the PATRIOT uses a total of six interconnecting cables, only three interconnecting wires were used in the model. (The effect of this use is discussed in sect. 4.8.) Each of the vehicles was grounded by an attached wire simulating a ground rod. Current probes (Tektronix CT-1 Current Transformer) were attached at the designated test points, and the center of rotation of the model was selected.

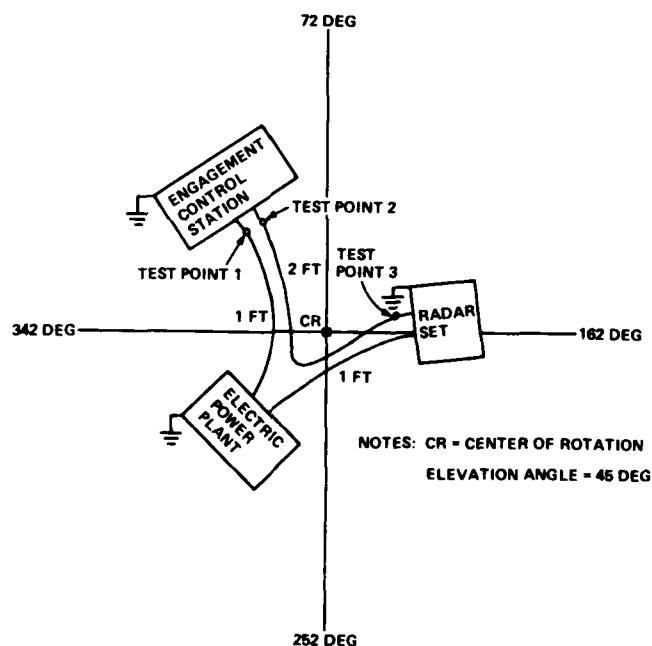


Figure 6. Configuration 1.

A center of rotation of the model was selected for each model configuration. The LDP was attached to a rotating support structure such that the antenna's bicone apex was 3 m from the center of rotation. The LDP was then rotated about the model, the azimuth being varied and the same slant range and angle of incidence being maintained. In this manner, the response of each test point was observed for 360 deg of antenna rotation. Response was measured typically at increments of 18 deg.

System configuration 1 did not include the AMG.

4.1.2 System Configuration 2

In configuration 2, the RS was removed along with its interconnecting wires to the ECS and the EPP (fig. 7). The current at test point 1 near the ECS was observed for 360 deg of azimuthal variation and recorded every 18 deg.

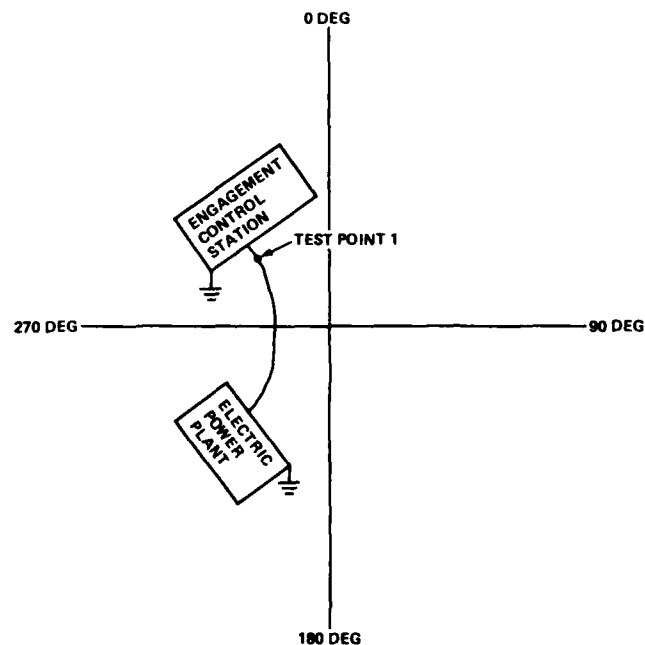


Figure 7. Configuration 2.

4.1.3 System Configuration 3

The azimuth angle was not varied in configuration 3, but the effects of special conditions were observed while the LDP was held at 0-deg azimuth and 45-deg elevation. Configuration 3 had the system interconnecting wire lengths of 2 ft each (fig. 8). In this configuration, there is more space between the wires than in configuration 1 so that the system looks more like a Δ than a Y. The current at test point 2 (at the RS) was observed under the normal condition (ground at the RS), with the RS ground removed, and finally with the RS removed. The current at test point 3 (at the EPP) was recorded with conditions normal or all grounds, wires, and vehicles attached.

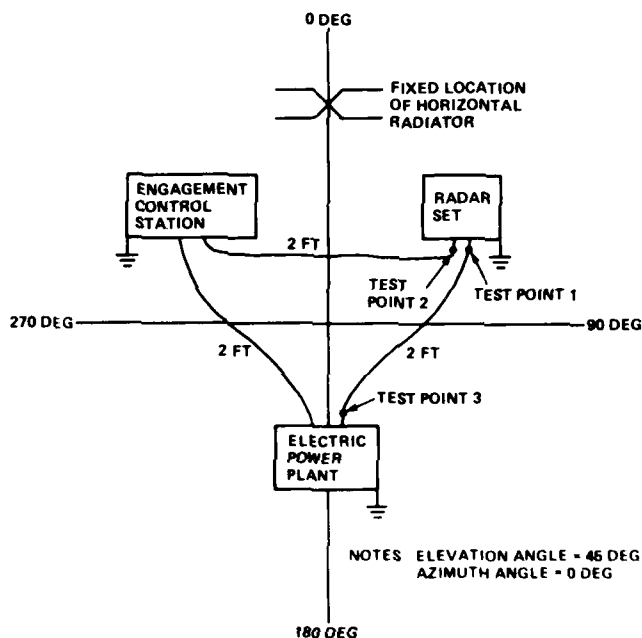


Figure 8. Configuration 3.

4.1.4 System Configuration 4

In configuration 4, the wire from the ECS to the RS was increased in length so that the model looked more like a Y than a Δ (fig. 9). With grounds at all three vehicles, the current at each of the three test points was observed for elevation angle = 45 deg and azimuth angle = 0 deg.

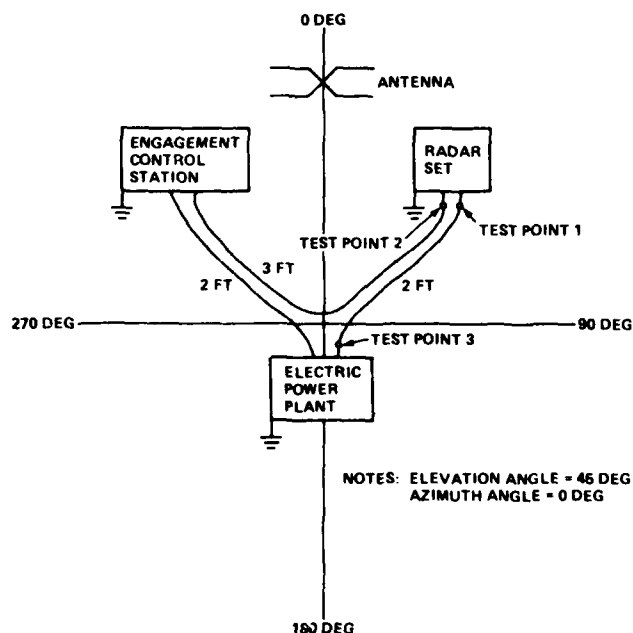


Figure 9. Configuration 4.

4.1.5 System Configuration 5

For configuration 5, the wires were laid to minimize the spacing between them (fig. 10). The currents at test points 1 to 3 were recorded in 18-deg increments for 360 deg of azimuth. The only ground was on the EPP.

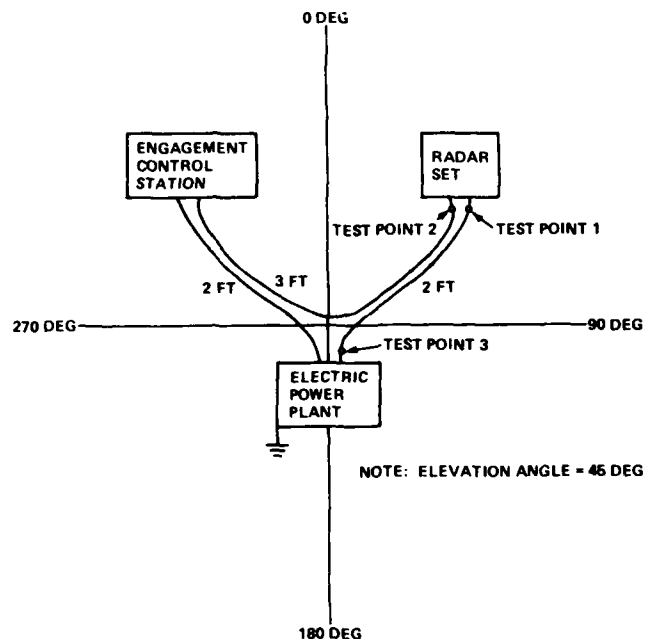


Figure 10. Configuration 5.

4.1.6 System Configuration 6

For configuration 6, current was measured at test points 2 and 3 for 360 deg of azimuthal change in 18-deg increments. The difference there was that the grounds were replaced (fig. 11, p. 24) on the ECS and the RS. These two test points can be compared with those in configuration 5 to observe the effects of the vehicle grounds and with those in configuration 4 to observe the effect of wire separation.

4.1.7 System Configuration 7

Configuration 7 (fig. 12) is almost identical to configuration 1 with the exception of a 1-ft-long wire running away from the EPP to a ground. This experiment was performed to observe the effect of having the local/remote unit (LRU) attached to the model. All three test points were observed at 18-deg increments for 360 deg of azimuthal variation with the LDP at 45-deg elevation.

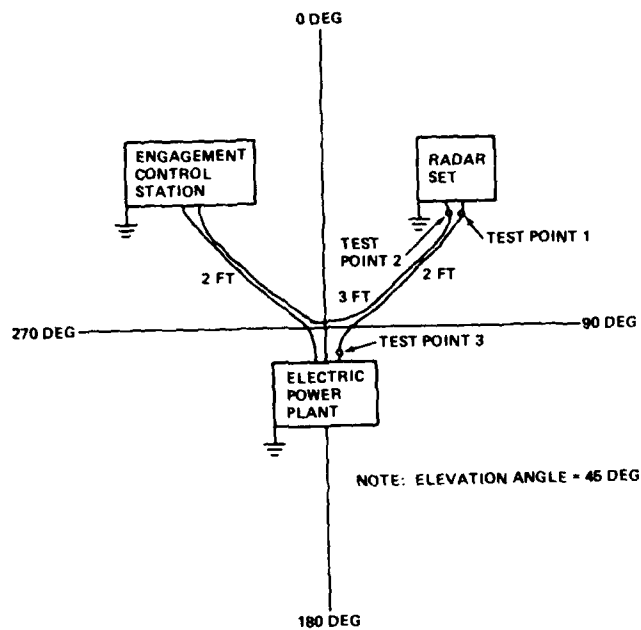


Figure 11. Configuration 6.

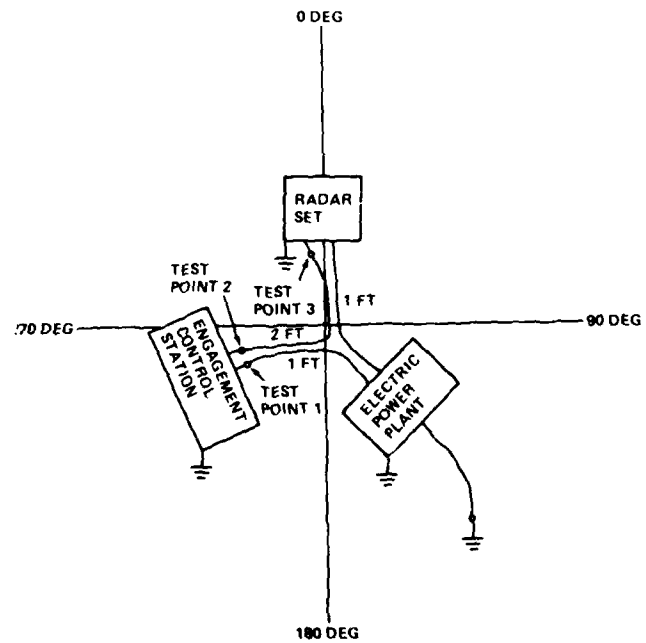


Figure 12. Configuration 7.

4.1.8 System Configuration 8

Configuration 8 was the same as configuration 7 with the addition of the AMG. This setup was used to observe the change in current at the ECS (fig. 13) when the angle of incidence was varied. As noted in table 2, 288 deg was selected as the azimuthal angle for these recordings. Elevation angles of 10, 20, 45, and 70 deg were recorded for test points 1 and 2 on the ECS.

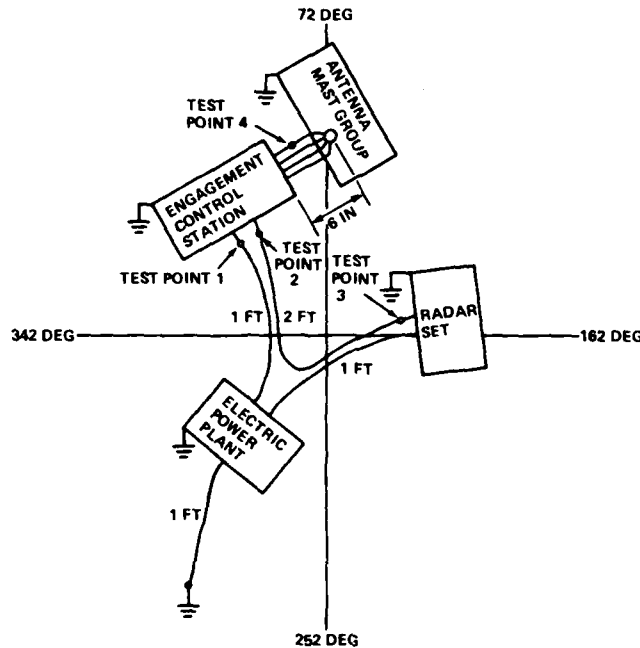


Figure 13. Configuration 8.

4.1.9 System Configuration 9

The PATRIOT model was illuminated vertically in configuration 9 (fig. 14). Currents were observed on the down leads of the AMG, on the wires coupling the AMG to the ECS, with and without the AMG attached, and with and without the AMG grounded. Some of these measurements were made for more than one azimuthal angle.

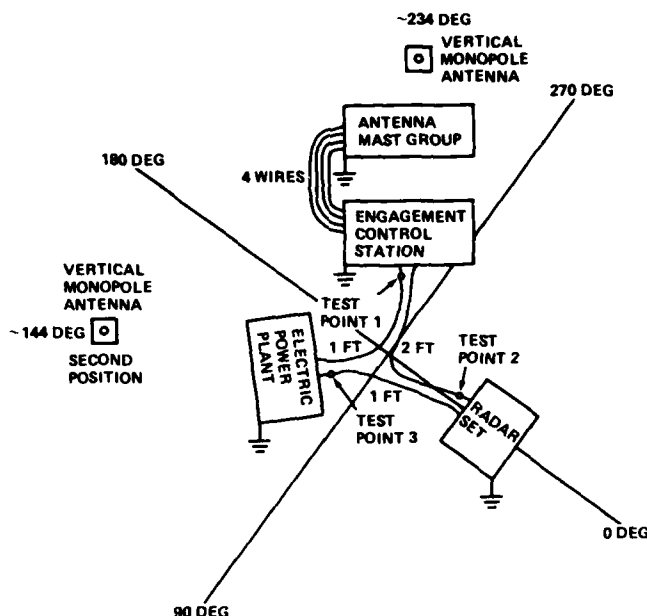


Figure 14. Configuration 9.

4.1.10 Measurement System Noise

Measurement system noise was observed by recording the response of a current probe with and without a PATRIOT system wire running through the probe while the test area was illuminated by the LDP. Current probes were physically reversed on the wires during initial setup to assure that the observed signals would reverse. All signals measured were significantly above the noise.

4.2 Horizontal Polarization Data

In conducting this scale-model test of the PATRIOT air defense system, more than 300 pieces of data were collected and are presently filed on magnetic discs. Only representative data are presented in this report for specific comparisons (see fig. 15, for example); all of the actual data are not included. Detailed analyses of specific waveforms can be relatively easy. One purpose of this task was to observe how the PATRIOT external receptor currents change with the variation of the arrival angles of the incident EMP. Therefore, a means of presenting this information was devised that graphically displays test point amplitude versus azimuth.

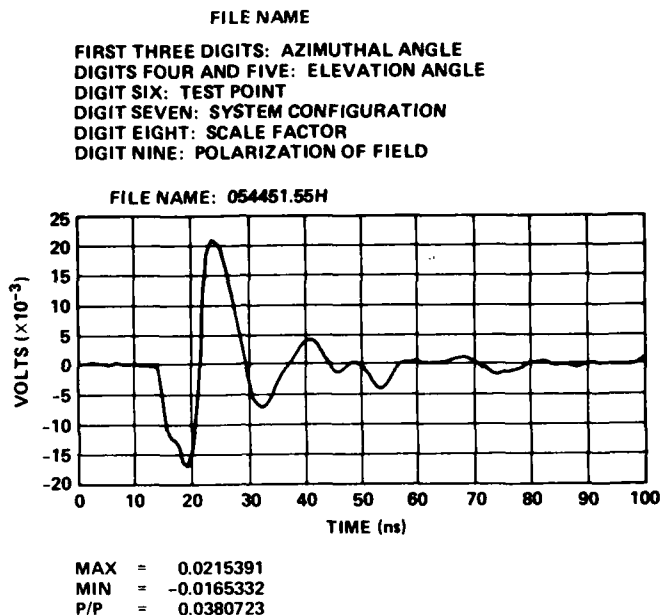


Figure 15. Explanation of file name and example of data.

In section 4, all the data are presented for relative comparison. Consequently, the units on the histograms and time domain plots are those of the recording instrument and not units of current.

The individual data representing the response of a given test point were recorded on magnetic (floppy) discs. In some cases, data were stored for each 18-deg increment so that the response of the test point was described for 360 deg of azimuth for a fixed angle of incidence. The computer of the Electromagnetic Scale Modeling Facility was programmed to operate on such data. Through it, the response of a test point can be plotted in two forms, as seen in figures 16 and 17.

Figure 16 is a histogram that shows the peak to peak variation of test point 1 as the azimuth of the model simulator was varied from 18 to 360 deg while the model was in system configuration 1. The plotted values are in millivolts and are proportional to the actual probe peak to peak amplitude response as recorded at the DPO. To convert to current, these values must be multiplied by 4 to account for the loss of the delay lines and also multiplied by the factor mA/5 mV to account for the current probe. Combining these two factors yields 0.8 mA/mV as a multiplication factor to yield milliamperes of current (peak to peak).

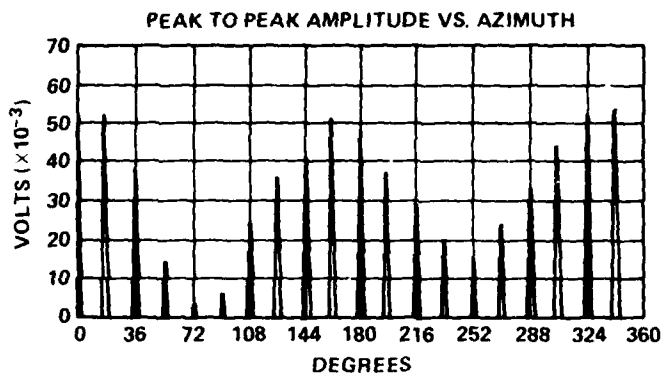


Figure 16. Configuration 1 histogram for test point 1: azimuth angle = 0 deg, elevation angle = 45 deg, and polarization = horizontal.

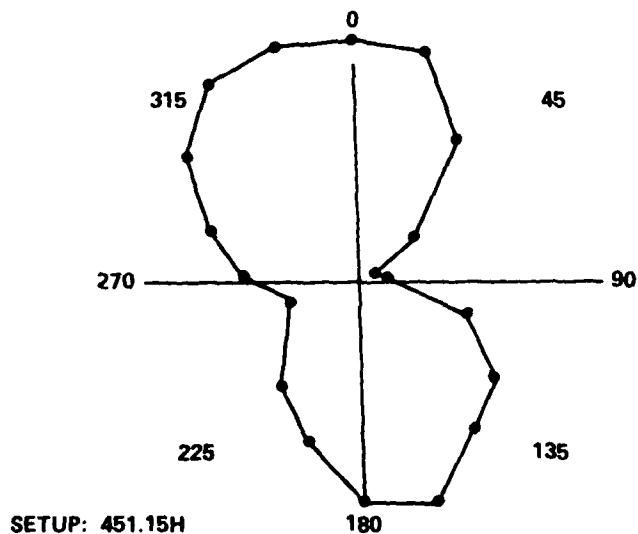
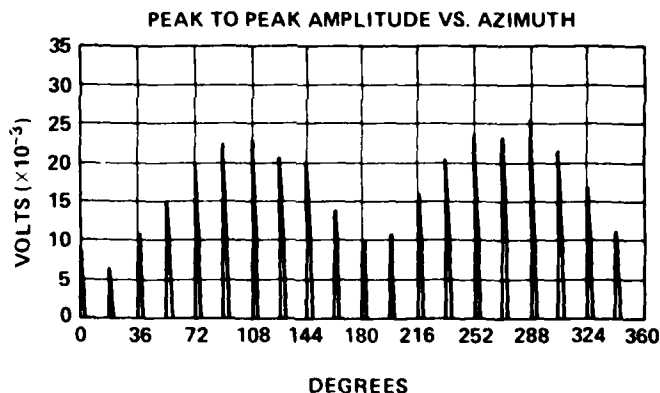


Figure 17. Configuration 1 polar plot for test point 1: elevation angle = 45 deg and polarization = horizontal.

This same factor (0.8 mA/mV) can be used to scale all the histograms and the time domain plots in this section from millivolts to milliamperes.

Figure 17 uses the histogram data in a different format. In this format, the computer has taken each of the 20 amplitudes and normalized them to the highest value found. The results are then plotted in a polar form that simultaneously displays how the test point current changes with azimuthal variation of the arriving wave. In effect, this plotting yields what may be thought of as a radiation pattern of the test point. These patterns allow one to quickly determine the direction from which maximum or minimum currents would be induced at that point of the PATRIOT for the given system configuration.

This process was repeated for test points 2 and 3 and may be viewed in figures 18 to 21. Referring to the polar plots for the three test points (fig. 17, 19, 21), it can be seen that for test point 1, where the wire follows a gentle curve, maximum current is at broadside illumination as one might expect. For test points 2 and 3, where the wire makes an approximate 90-deg bend, intuition cannot be trusted.



000452.15H

MAX = 0.0251 V AT 288 DEG

Figure 18. Configuration 1 histogram for test point 2: elevation angle = 45 deg and polarization = horizontal.

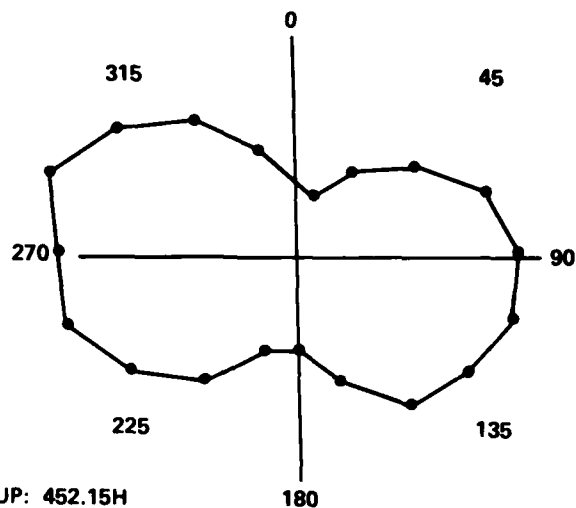


Figure 19. Configuration 1 polar plot for test point 2: elevation angle = 45 deg and polarization = horizontal.

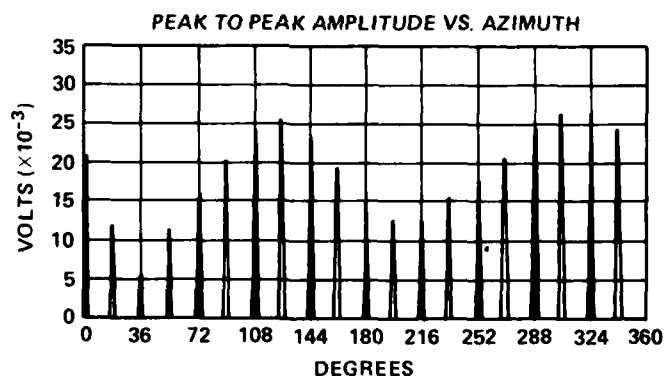


Figure 20. Configuration 1 histogram for test point 3: elevation angle = 45 deg and polarization = horizontal.

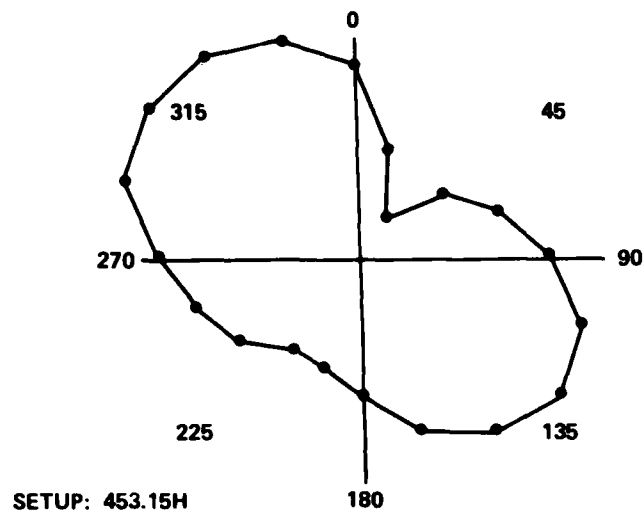
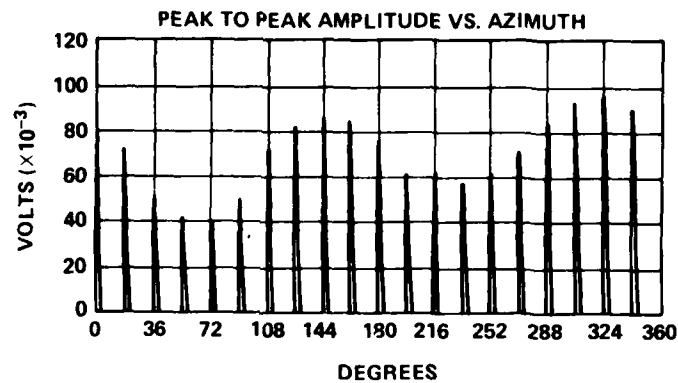


Figure 21. Configuration 1 polar plot for test point 3: elevation angle = 45 deg and polarization = horizontal.

Since the computer operates on stored data that are easily and quickly retrieved, yet another graphic display was devised for presenting the PATRIOT model's external receptor responses. In viewing the previous polar plots of test points 1 to 3 (fig. 17, 19, 21), it is apparent that each of them has a different azimuthal angle of maximum response. If one were to view all three plots, it could be visualized that the overall maximum system response occurs in the 270- to 360-deg quadrant. To graphically display this overall response, the responses of all three test points were added together in the computer. The result is displayed in histogram form (fig. 22) and as a polar plot (fig. 23), where all points are normalized to the highest value. If these test points are considered as adequately defining the coupling to the system, then 324 deg would represent the azimuthal angle of maximum coupling.

The PATRIOT model was tested in this manner in two other configurations. In system configurations 5 and 7, the responses of three test points were observed for 360 deg of simulator azimuthal variation. Figures 24 and 25 show the plan view of configurations 5 and 7, respectively. Figures 26 to 28 show the histograms of the peak to peak amplitudes of the currents for test points 1 to 3 for configuration 5, and figures 29 to 31 show the normalized polar plots. Figures 32 to 34 are the histograms and figures 35 to 37 are the polar plots for configuration 7.



MAX = 0.0957 V AT 324 DEG

Figure 22. Superposition of configuration test points 1, 2, and 3 in histogram form: elevation angle = 45 deg and polarization = horizontal.

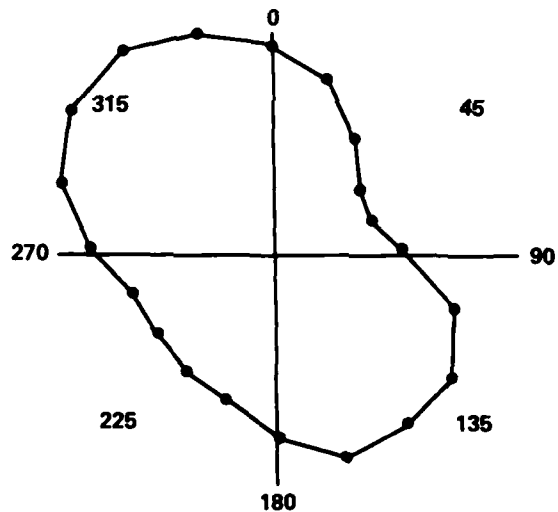


Figure 23. Superposition of configuration test points 1, 2, and 3 in polar form: elevation angle = 45 deg and polarization = horizontal.

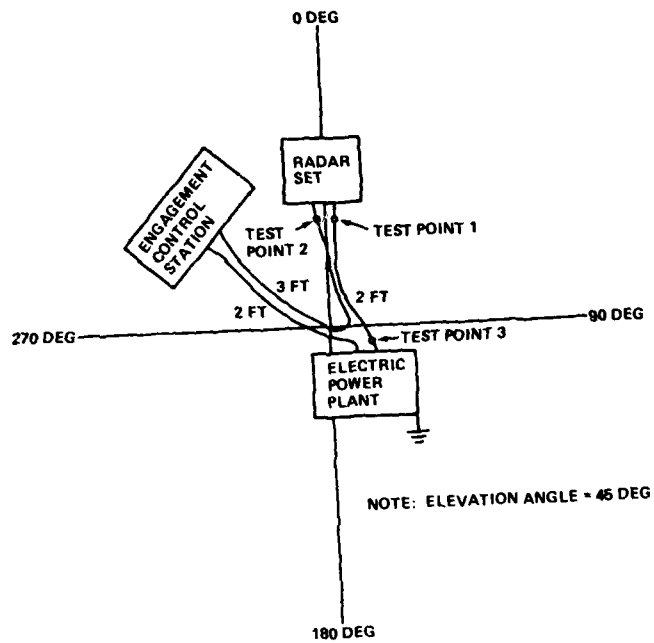
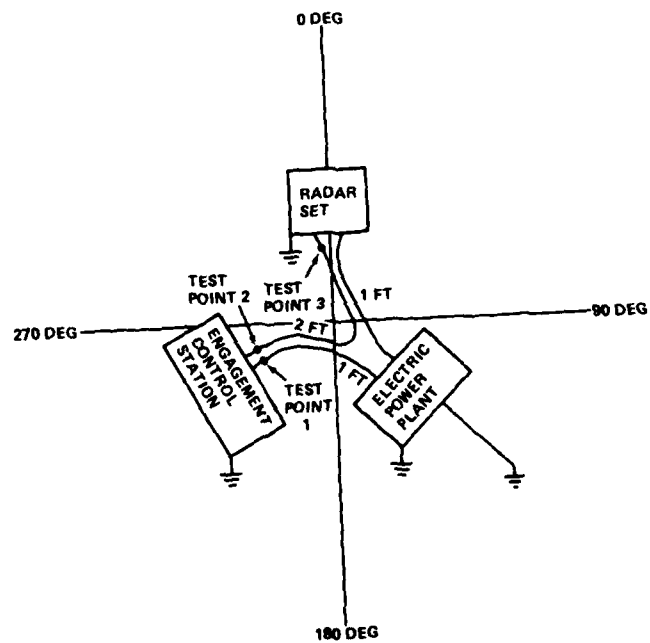
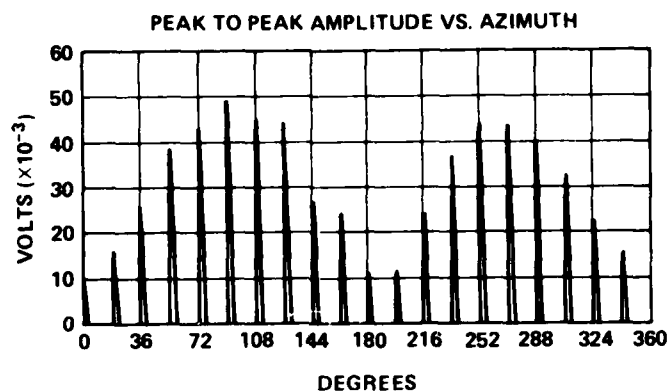


Figure 24. Configuration 5:
plan view.

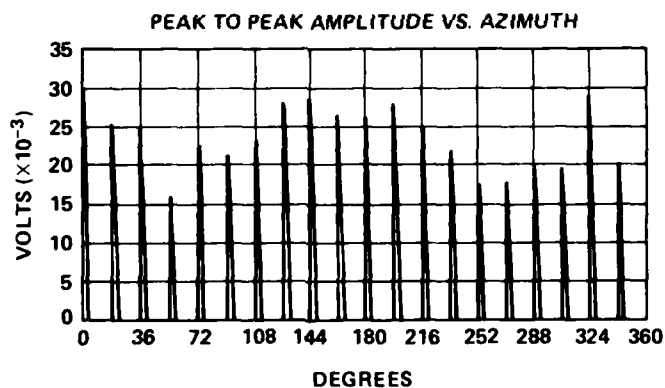
Figure 25. Configuration 7:
plan view.





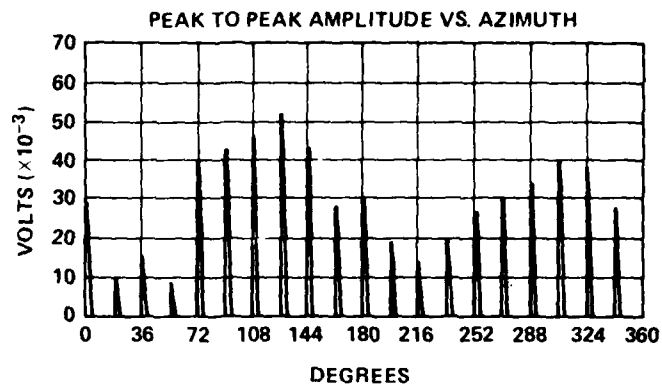
000451.55H
MAX = 0.049 V AT 90 DEG

Figure 26. Configuration 5 histogram for test point 1: elevation angle = 45 deg and polarization = horizontal.



000452.55H
MAX = 0.0295 V AT 0 DEG

Figure 27. Configuration 5 histogram for test point 2: elevation angle = 45 deg and polarization = horizontal.



000453.55H

MAX = 0.052 V AT 126 DEG

Figure 28. Configuration 5 histogram for test point 3: elevation angle = 45 deg and polarization = horizontal.

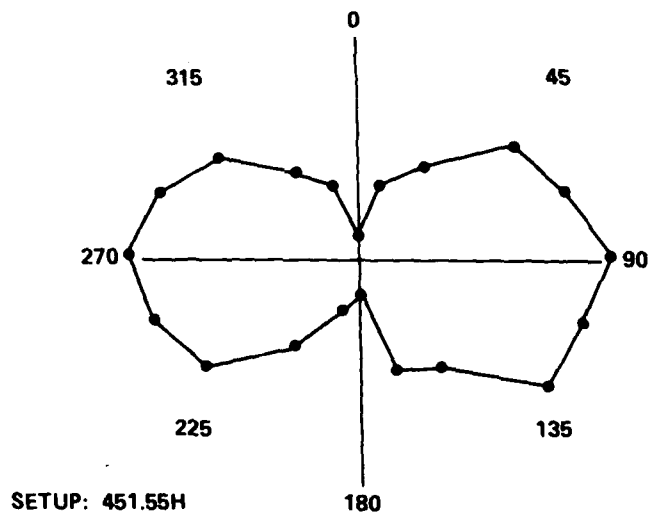


Figure 29. Configuration 5 polar plot for test point 1: elevation angle = 45 deg and polarization = horizontal.

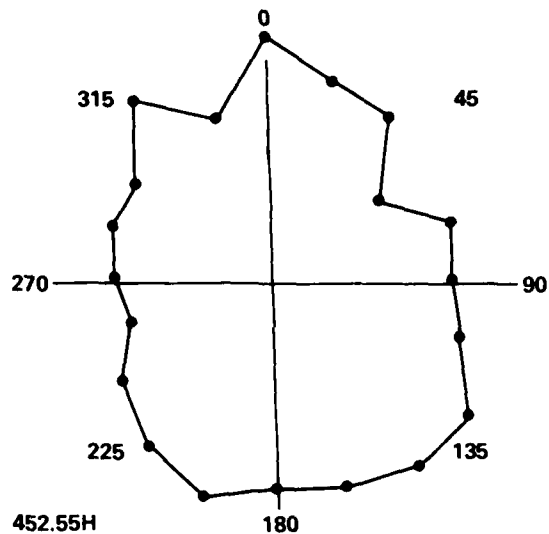


Figure 30. Configuration 5 polar plot for test point 2: elevation angle = 45 deg and polarization = horizontal.

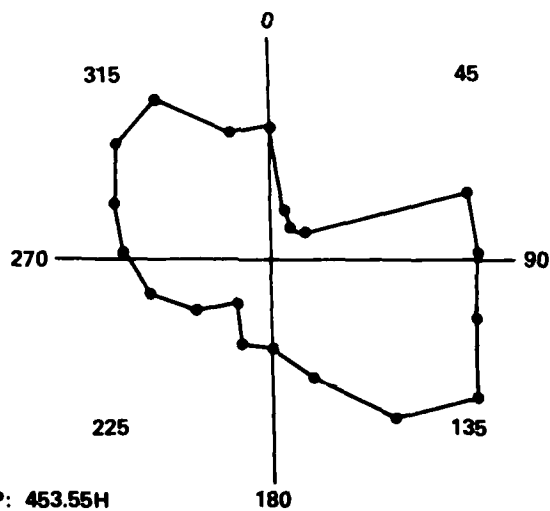
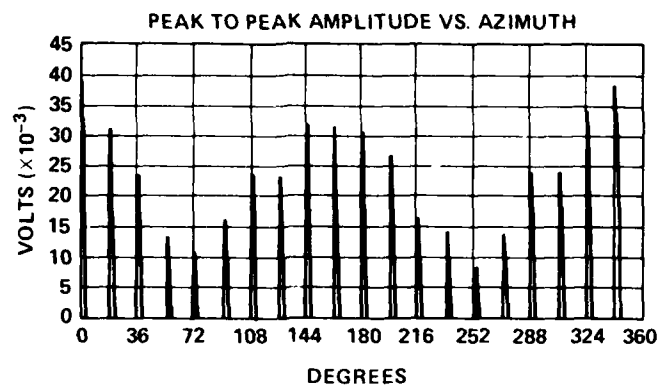
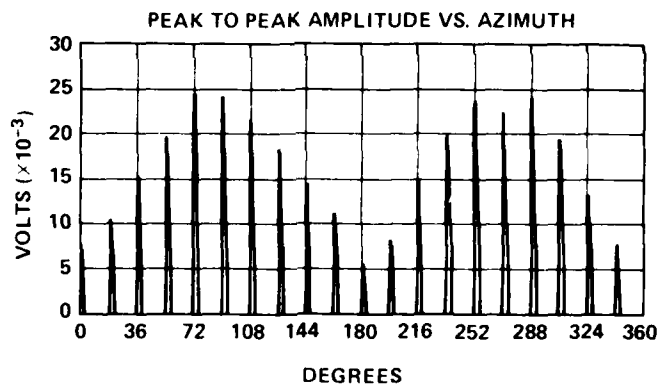


Figure 31. Configuration 5 polar plot for test point 3: elevation angle = 45 deg and polarization = horizontal.



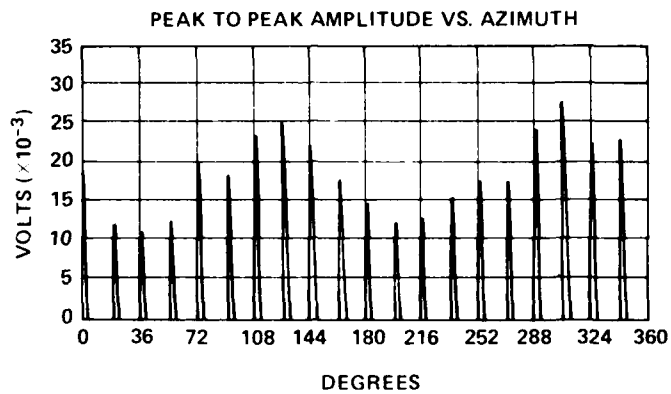
000451.75H
MAX = 0.0386 V AT 0 DEG

Figure 32. Configuration 7 histogram for test point 1: elevation angle = 45 deg and polarization = horizontal.



000452.75H
MAX = 0.0242 V AT 72 DEG

Figure 33. Configuration 7 histogram for test point 2: elevation angle = 45 deg and polarization = horizontal.



000453.75H
 MAX = 0.0274 V AT 306 DEG

Figure 34. Configuration 7 histogram for test point 3: elevation angle = 45 deg and polarization = horizontal.

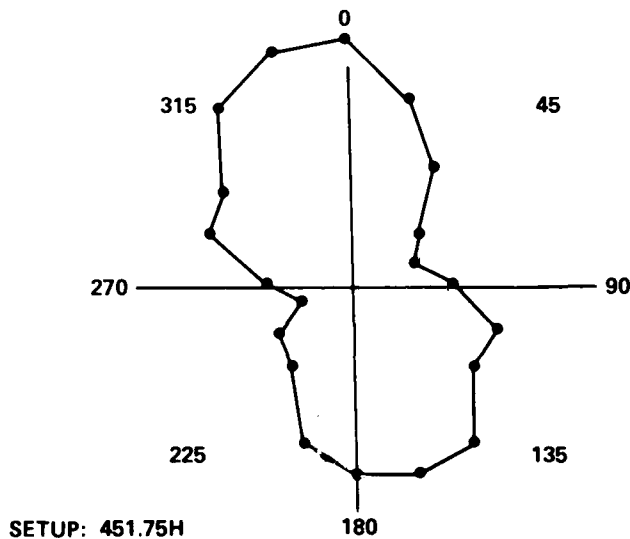


Figure 35. Configuration 7 polar plot for test point 1: elevation angle = 45 deg and polarization = horizontal.

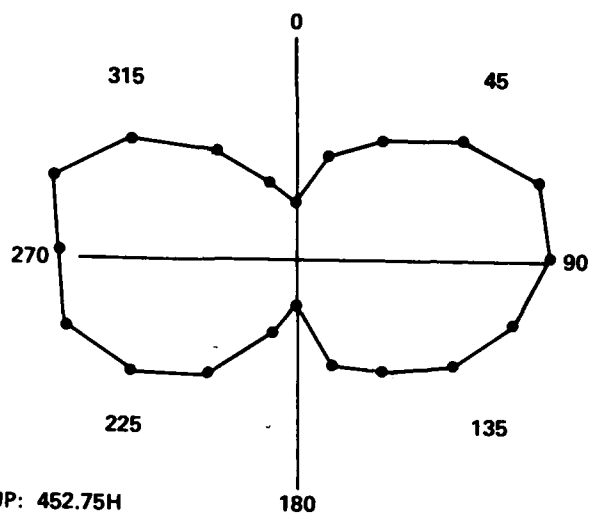


Figure 36. Configuration 7 polar plot for test point 2: elevation angle = 45 deg and polarization = horizontal.

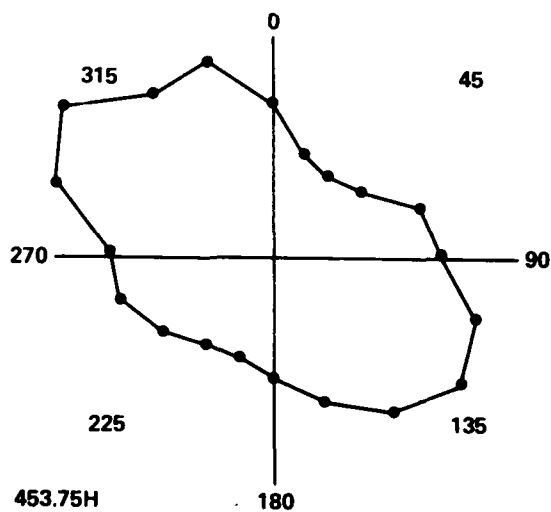


Figure 37. Configuration 7 polar plot for test point 3: elevation angle = 45 deg and polarization = horizontal.

Table 2 shows the results of the variation of angle of elevation on test points 1 and 2 (configuration 8). The effect of the AMG and AMG to ECS wire was not observed to strongly influence the coupling to the remainder of the system for this azimuthal angle. Section 4.6 examines a case where the AMG to ECS wire current does couple strongly to the ECS to EPP wire.

TABLE 2. RESULTS OF SYSTEM CONFIGURATION 8
EXPERIMENT (AZIMUTH ANGLE = 288 DEG)

Test Point	Incidence angle (deg)	Amplitude peak to peak (mV)
1	10	21
	20	26
	45	27*
	70	58
2	10	16
	20	23
	45	32
	70	48

*Configuration 1: 32 mV.

4.3 Effects of Number of PATRIOT Vehicles

The PATRIOT model configuration 2 (fig. 38) was obtained from configuration 1 by the removal of the model RS and its coupling wires. The current measured in this configuration shows little difference in amplitude (fig. 39) and azimuthal distribution (fig. 40, p. 42) from those of the corresponding test point for configuration 1 (fig. 16, 17). This similarity indicates that, rather than responding to the vehicular loop, each test point in the model responds approximately as an isolated single wire loaded at its terminations essentially by the capacitive coupling of the vehicles to ground.

4.4 Effects of Vehicle Grounds

A possible field deployment of the PATRIOT would be with only one of the FCS vehicles grounded. The data from model configuration 5 (fig. 24) shows the current versus azimuth on the RS to ECS wire (fig. 27, 30) and on the EPP to RS wire (fig. 28, 31) when there were no grounds on either the ECS or the RS. Model configuration 6 data were

collected for these wires with the grounds in place on the ECS and the RS. The RS to ECS wire responses are figure 41 (histogram) and figure 42 (polar plot), and figures 43 and 44 represent the EPP to RS responses. Although there are some differences with and without grounds, they are not dramatic.

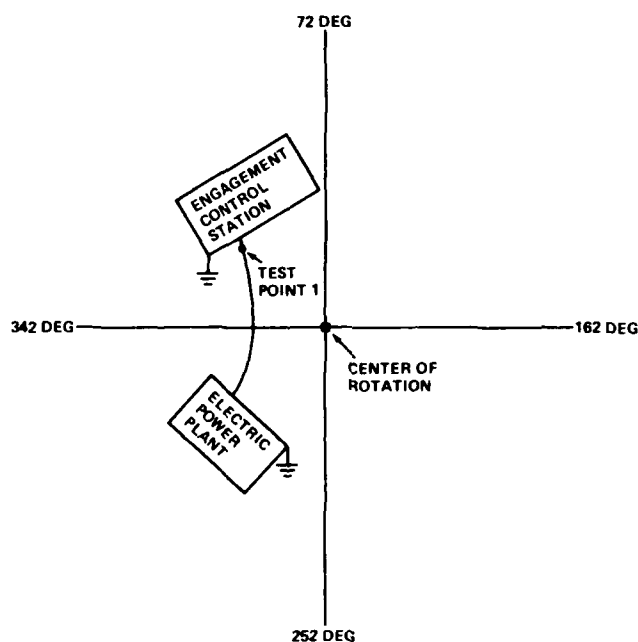
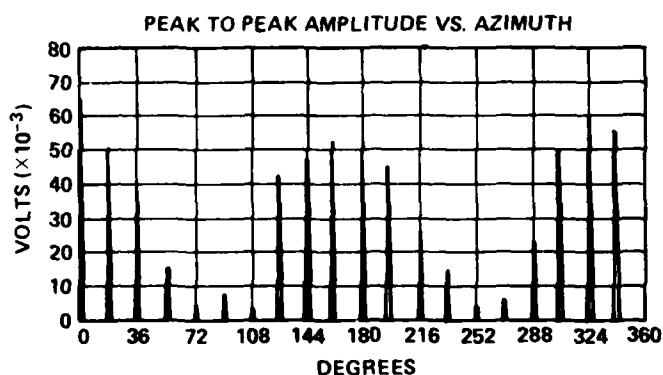


Figure 38. Configuration 2, showing center of rotation.

Figure 39. Configuration 2 histogram for test point 1: elevation angle = 45 deg and polarization = horizontal.



000451.25H
MAX = 0.0647 V AT 0 DEG

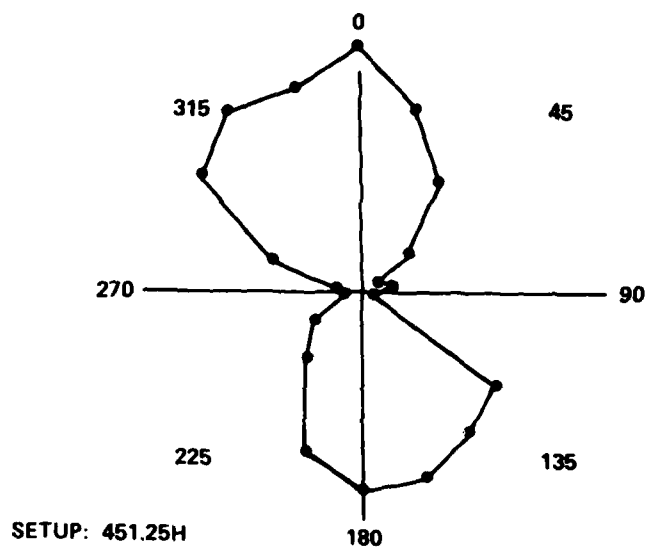
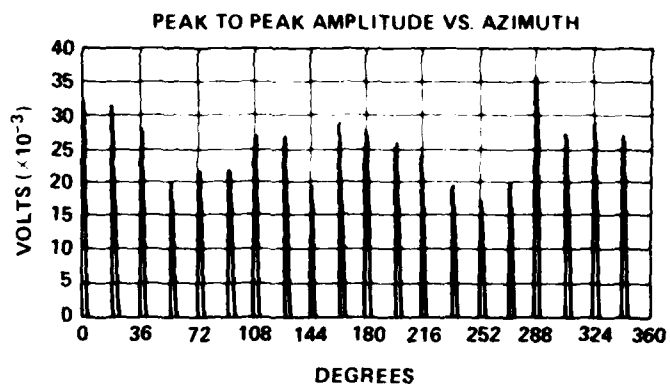


Figure 40. Configuration 2 polar plot for test point 1: elevation angle 45 deg and polarization = horizontal.



000452.65H
MAX = 0.0344 V AT 288 DEG

Figure 41. Configuration 6 histogram for test point 2: elevation angle = 45 deg and polarization = horizontal.

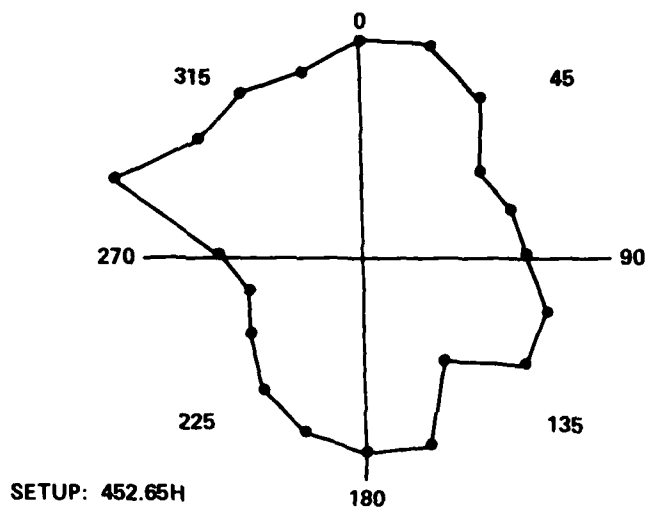
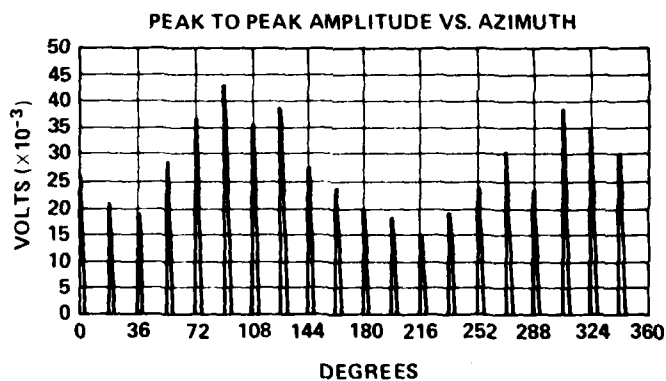


Figure 42. Configuration 6 polar plot for test point 2: elevation angle = 45 deg and polarization = horizontal.



000453.65H
MAX = 0.0431 V AT 90 DEG

Figure 43. Configuration 6 histogram for test point 3: elevation angle = 45 deg and polarization = horizontal.

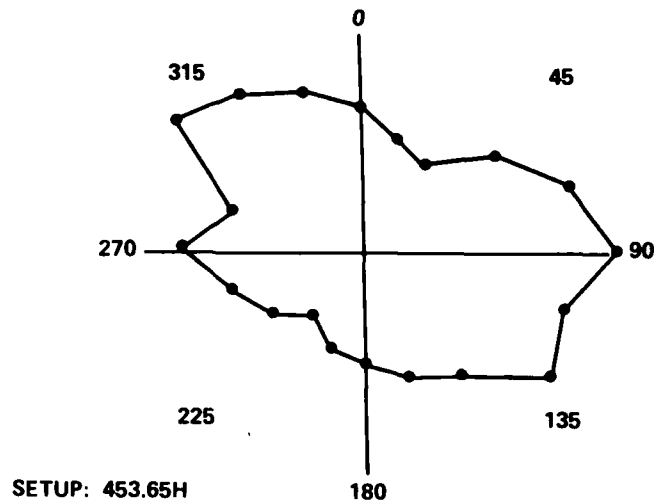


Figure 44. Configuration 6 polar plot for test point 3: elevation angle = 45 deg and polarization = horizontal.

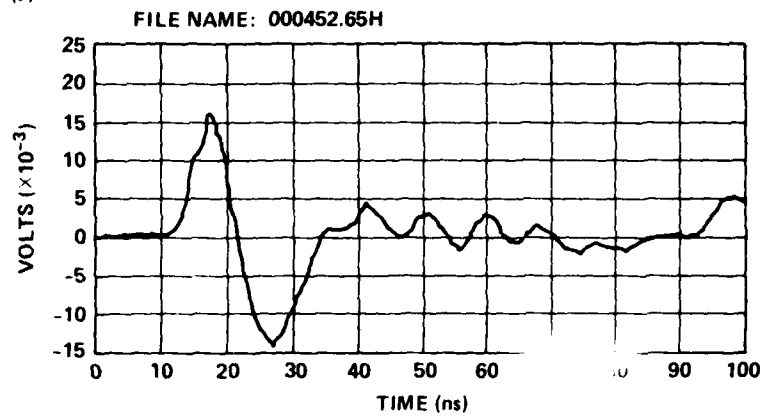
4.5 Effects of Cable Routing

The currents induced in the external receptors of the PATRIOT change with the routing of receptors. The proximity of the receptors was intentionally changed to observe these effects (fig. 9, 11). The currents in tightly coupled configuration 6 (fig. 45) were observed to be one-third less than in loosely coupled configuration 4 (fig. 46, p. 46). Cable configurations are compared in tables 3 and 4 (p. 47). A tight Y configuration (6) seems to couple more to the incident field than a loose Y configuration (1) with shorter sides.

4.6 Coupling to ECS to EPP Cable with and without AMG and AMG to ECS Cable

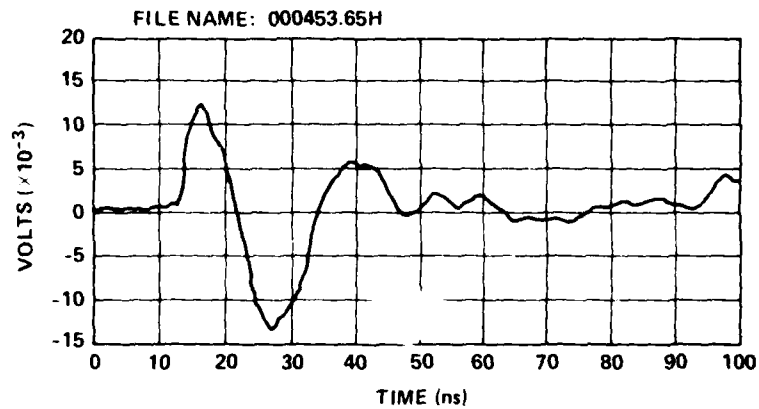
The purpose of another experiment was to determine the degree to which the AMG and AMG to ECS cable influences the coupling to the ECS to EPP cable. Shown in figure 47 are the configurations excited. The time domain waveforms at the test point are presented in figures 48 to 50. We see that the presence of the AMG and AMG to ECS wire definitely changes the waveform at the test point. In figure 50, the vertical mast was removed from the AMG to verify that indeed the coupling was to the horizontal AMG to ECS wire and not due to some spurious vertical field coupling to the mast.

(a)



MAX = 0.0189
MIN = 0.0112
P/P = 0.0301

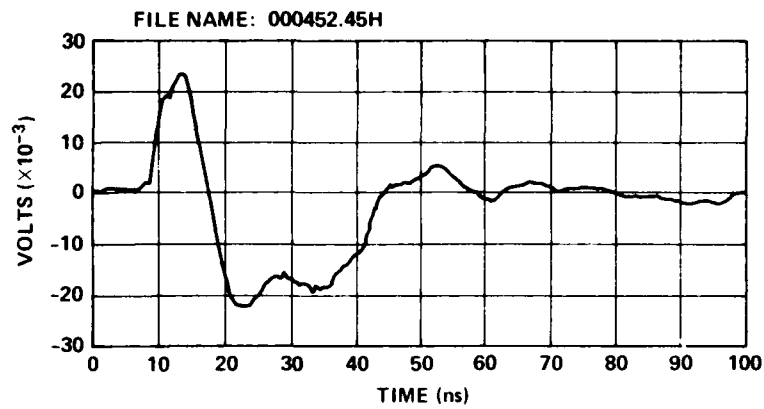
(b)



MAX = 0.0161
MIN = 9.4589×10^{-3}
P/P = 0.0256

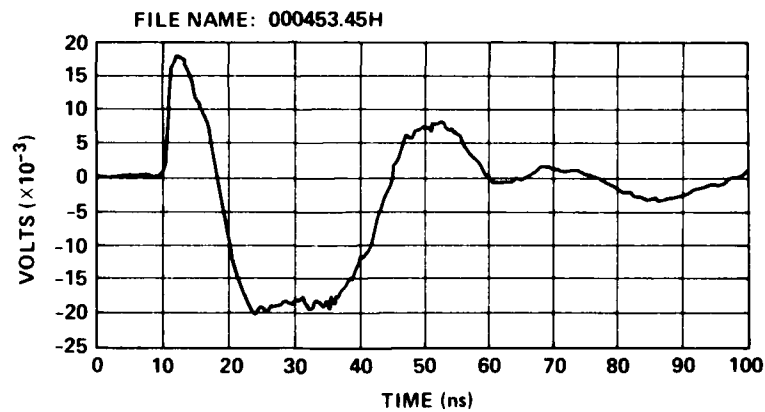
Figure 45. Effects of wire routing for configuration 6: elevation angle = 45 deg and polarization = horizontal: (a) test point 2 and (b) test point 3.

(a)



MAX = 0.0249
MIN = 0.0208
P/P = 0.0458

(b)



MAX = 0.0196
MIN = 0.0186
P/P = 0.0382

Figure 46. Effects of wire routing for configuration 4: elevation angle = 45 deg and polarization = horizontal: (a) test point 2 and (b) test point 3.

TABLE 3. CONFIGURATION 3 AND 4 RESPONSES

System Configuration	Wire spacing shape	Test point	Amplitude peak to peak (mV)
3	~Δ	1	11
		2	78
		3	40
4	Loose Y	1	9.5*
		2	46
		3	38

*No baseline.

TABLE 4. CONFIGURATION 1 AND 6 RESPONSES

System configuration	Wire spacing shape	Test point	Max amplitude peak to peak (mV)	Figure
1	Loose Y	1	54	16
		2	25	18
		3	26	20
6	Tight Y	2	35	41
		3	43	43

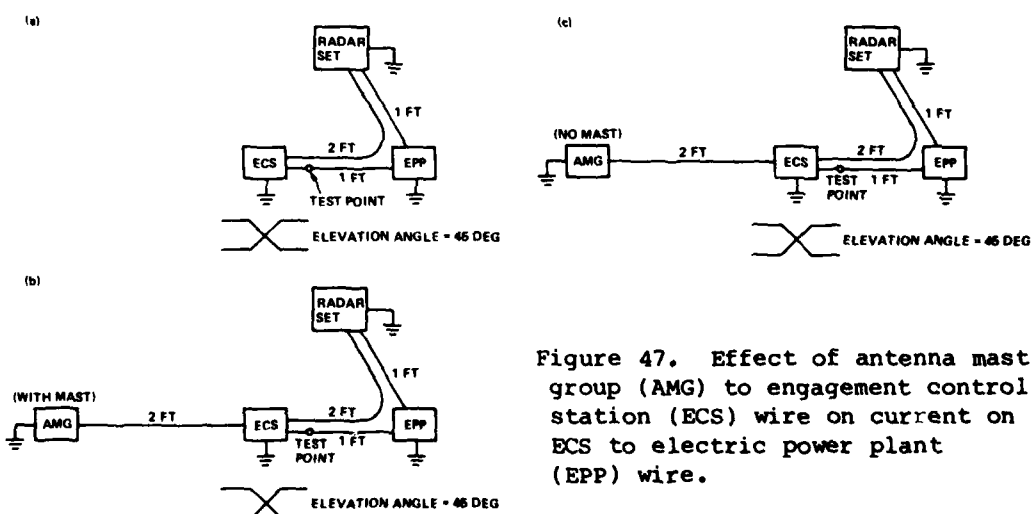


Figure 47. Effect of antenna mast group (AMG) to engagement control station (ECS) wire on current on ECS to electric power plant (EPP) wire.

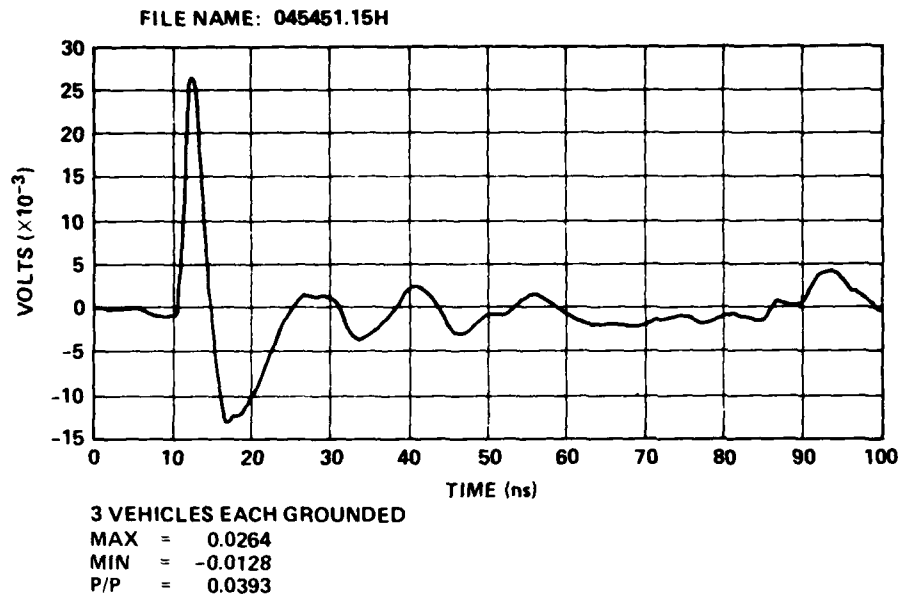


Figure 48. Test with antenna mast group to engagement control station wire for test point 1, three vehicles each grounded: azimuth angle = 45 deg and elevation angle = 45 deg (see fig. 47a).

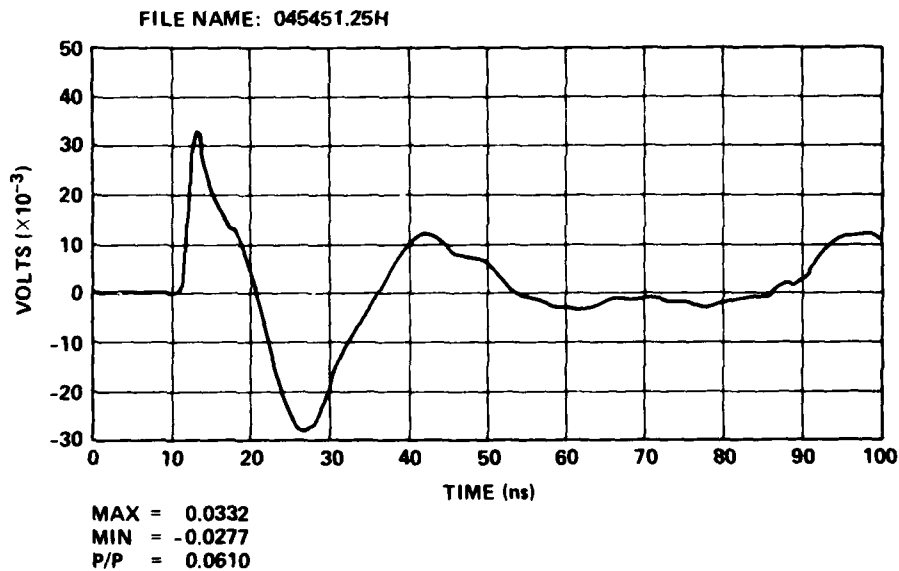


Figure 49. Test with antenna mast group (AMG) to engagement control station wire for test point 1, four vehicles each grounded and AMG attached: azimuth angle = 45 deg and elevation angle = 45 (see fig. 47b) (file name does not reflect correct configuration).

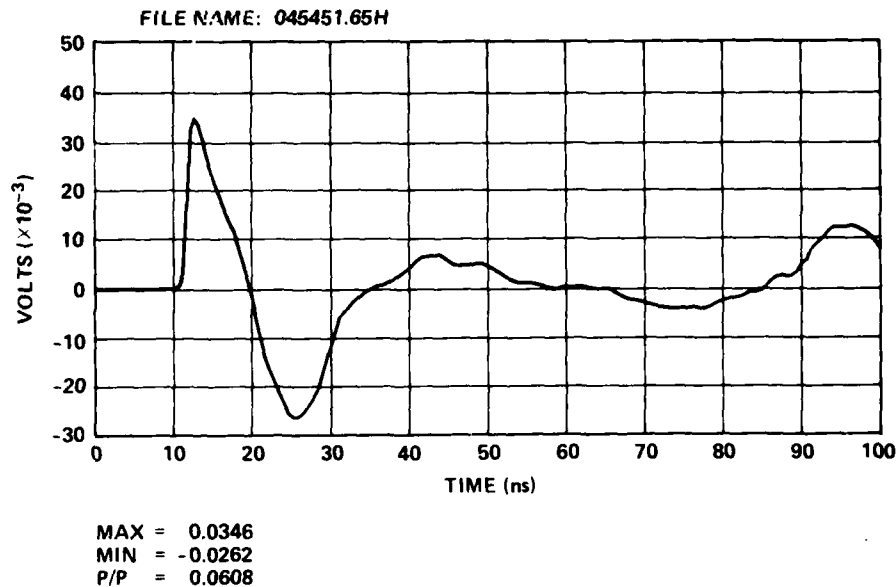


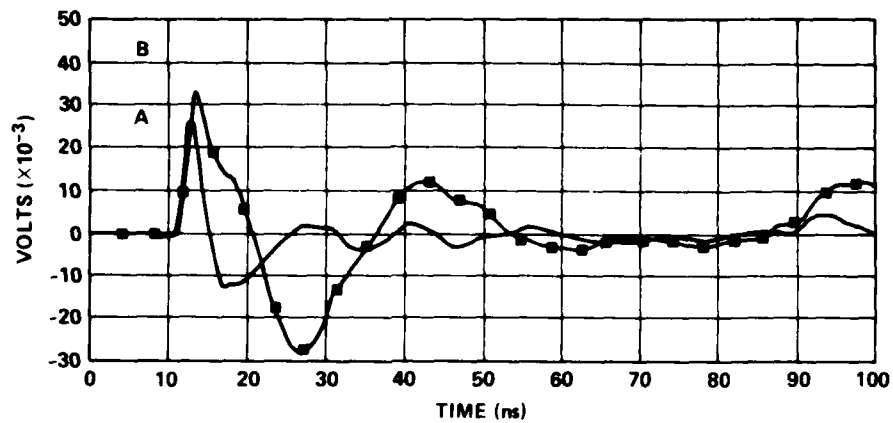
Figure 50. Test with antenna mast group (AMG) to engagement control station cable for test point 1, four vehicles all grounded and mast removed from AMG: azimuth angle = 45 deg and elevation angle = 45 deg (see fig. 47c) (file name does not reflect correct configuration).

Figures 48 and 49 are superimposed and replotted in figure 51 for ease of comparison. Figure 52 shows the superimposed FFT's of the waveforms shown in figure 51. There is a dramatic difference as seen in the FFT's. The addition of the AMG and AMG to ECS wire introduces considerable low-frequency energy below about 60 MHz in the model. This would be 60 MHz/50 or 1.2 MHz in the full-scale system (see p. 50 for fig. 51, 52).

Appendix B describes an experiment to determine the effect of removing the ECS on the current measured on the wire from the ECS to the EPP.

4.7 Angle of Incidence Variation

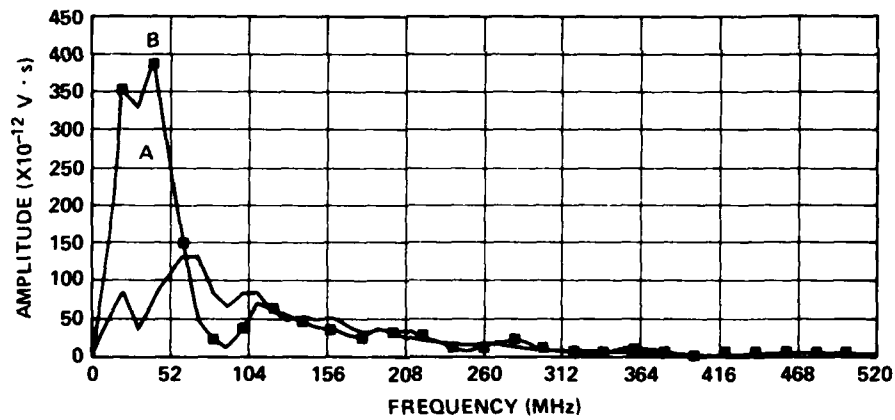
The current at the test point of the configurations shown in figure 53 was determined as a function of the angle of elevation measured with respect to the ground. The angles were 10, 45, and 90 deg. We compare waveforms for the two configurations in figures 54 to 56. The coupling increases with angle. In figure 57, the FFT's are compared for the loop configuration at 10 and 90 deg.



WAVEFORM A PATRIOT, 3 VEHICLES EACH GROUNDED
045451.15H

WAVEFORM B PATRIOT, 4 VEHICLES EACH GROUNDED, AMG ATTACHED
045451.25H

Figure 51. Waveforms of figures 48 and 49 superimposed.



FFT A PATRIOT, 3 VEHICLES EACH GROUNDED

FFT B PATRIOT, 4 VEHICLES EACH GROUNDED, AMG ATTACHED

Figure 52. Fast Fourier transforms of figure 51 waveforms.

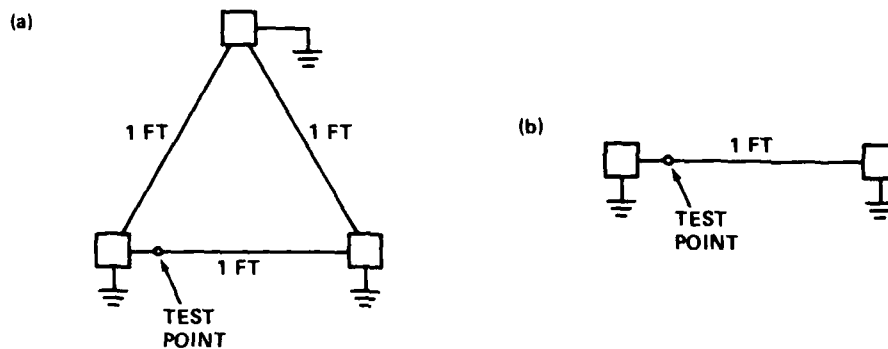
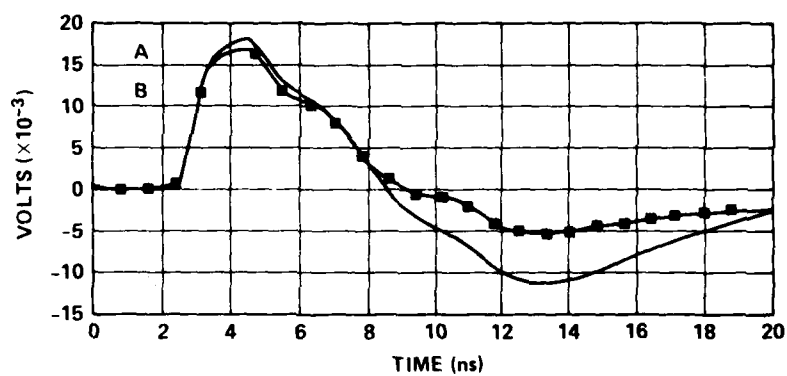


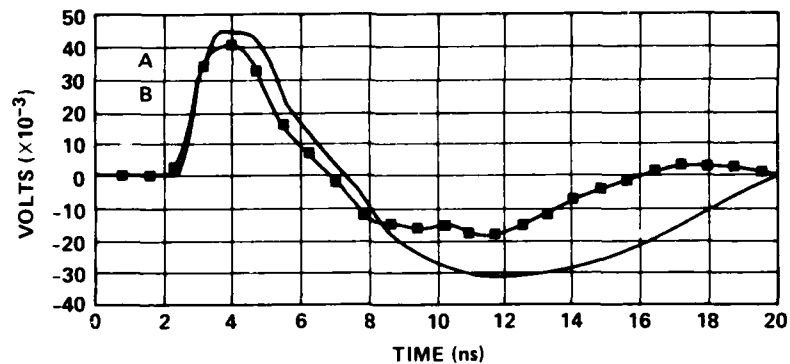
Figure 53. Configurations: (a) loop versus (b) two vehicles.



WAVEFORM A PATRIOT LOOP EXPERIMENT TWO VEHICLES ONE WIRE,
FILE NAME: JUNE15.7

WAVEFORM B PATRIOT LOOP EXPERIMENT, FILE NAME: JUNE15.6

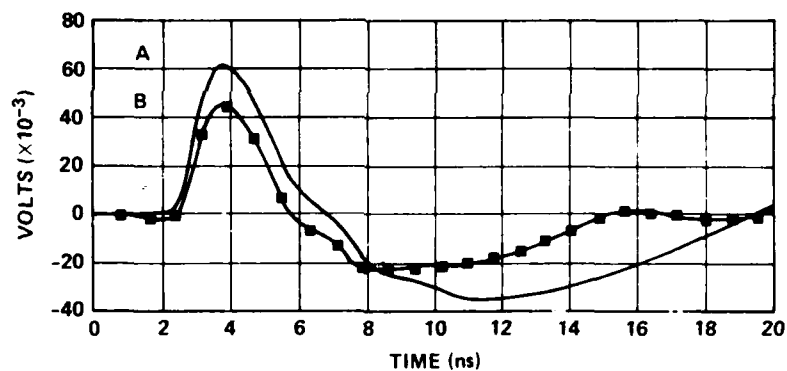
Figure 54. Loop versus two vehicles: 10-deg elevation angle.



WAVEFORM A PATRIOT LOOP EXPERIMENT TWO VEHICLES ONE WIRE,
FILE NAME: JUNE15.10

WAVEFORM B PATRIOT LOOP EXPERIMENT, FILE NAME: JUNE15.4

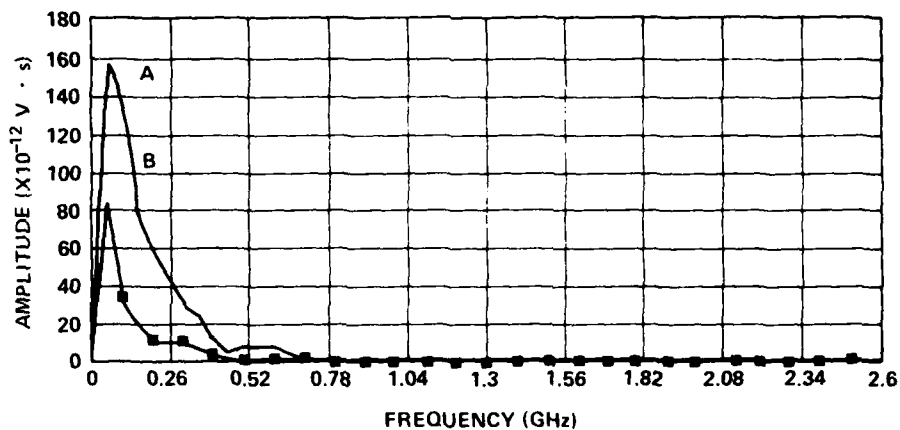
Figure 55. Loop versus two vehicles: 45-deg elevation angle.



WAVEFORM A PATRIOT LOOP EXPERIMENT TWO VEHICLES ONE WIRE,
FILE NAME: JUNE15.11

WAVEFORM B PATRIOT LOOP EXPERIMENT, FILE NAME: JUNF15.1

Figure 56. Loop versus two vehicles: 90-deg elevation angle.



FFT A PATRIOT LOOP EXPERIMENT
 MAX(A) IS AT 5×10^7 Hz, FILE NAME: JUNE15.1
 90 DEG

FFT B PATRIOT LOOP EXPERIMENT
 MAX(B) IS AT 5×10^7 Hz, FILE NAME: JUNE15.6
 10 DEG

Figure 57. Comparison of loop fast Fourier transforms for 90- and 10-deg angles of elevation.

4.8 Current Sharing on Parallel Conductors Illuminated by Electromagnetic Wave

When parallel conductors lying on the ground are illuminated by an electromagnetic wave, the current induced on any one of the conductors is a function of the separation of the conductors. It was anticipated that the current induced on any given conductor would be a maximum when the separation distance between the conductors was large enough to effectively decouple them. To investigate this current sharing phenomenon, two vehicles with grounds were connected with one to three wires at 1-in. (2.54-cm) and 1/8-in. (0.32-cm) separations.

First the current in a single wire was recorded; then another wire was brought up close, and the current was measured again. Next another wire was brought up, totaling three wires, with the monitored wire (carrying the current) in the center. The current was measured both in the center and at the end (near the vehicle). The current at the end was 64 percent of that at the center for the three-wire cases, 65 percent of the end current for the two-wire case, and 79 percent of the end current for the one-wire case.

The results of the current sharing experiment are shown in table 5. The current on the wire monitored decreased as the number of wires was increased and the separation between wires was reduced.

TABLE 5. CURRENT SHARING EXPERIMENTAL DATA

Normalization to one-wire case (amplitude peak to peak)	Placement of current probe		
	In center		Near vehicle, wire separation 1 in.
	Wire separation 1 in.	Wire separation 1/8 in.	
Current (two wires)/current (one wire)	0.66	0.56	0.54
Current (three wires)/current (one wire)	0.42	0.29	0.30

4.9 Vertical Polarization Data

The response of the PATRIOT model to a vertical illumination was observed by using model configuration 9 (fig. 14). Data were collected from three test points by using two source azimuths and three configurations. These configurations were with the AMG attached and all four vehicles grounded, with the AMG attached and it alone not grounded, and with no AMG or associated wires present with the three vehicles grounded. The data are presented in figures 58 to 76, and the peak to peak values are listed in table 6 (p. 64).

As one might expect, the attachment of the AMG increases the current at the ECS, the most closely coupled vehicle. In general, the addition of the AMG causes the current at the radar set to remain the same or to go down, while the power plant current is essentially unaffected. Clearly, grounding the AMG reduces the currents induced in the model by a vertical field.

It is interesting to observe that there is strong vertical coupling to the system even without a dominant vertical member like the AMG mast.

4.10 Comparison of Horizontal and Vertical Data

The PATRIOT model was illuminated by using both horizontal and vertical pulse radiators. Since the field strengths from both of these sources were within 15 percent (99 V/m vertically and 87 V/m horizontally), it is possible to directly compare the response of a test point to both sources with small error. Figure 76 shows the current

recorded at the ECS for both vertical (a) and horizontal (b) illumination. The model was in the same configuration for both of these waveforms (no AMG was present in either illumination). The waveforms of these currents differ only somewhat. The peak to peak amplitude of the horizontal response is approximately twice that of the vertical response. Appendix C compares the response of a wire above the ground to a horizontally and vertically polarized incident field.

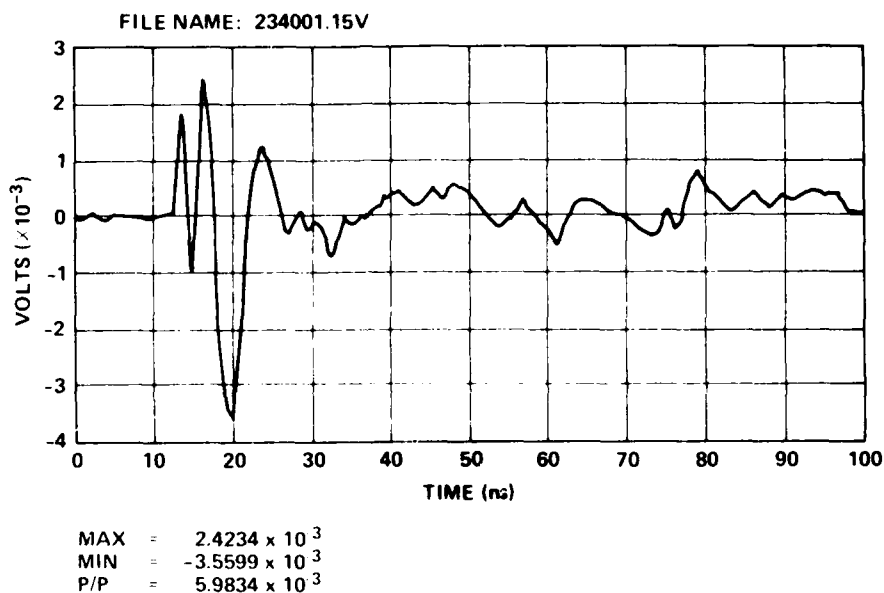


Figure 58. Configuration 9 vertical polarization experiment, test point 1, three vehicles, no antenna mast group: azimuth angle = 234 deg (file name does not reflect correct configuration).

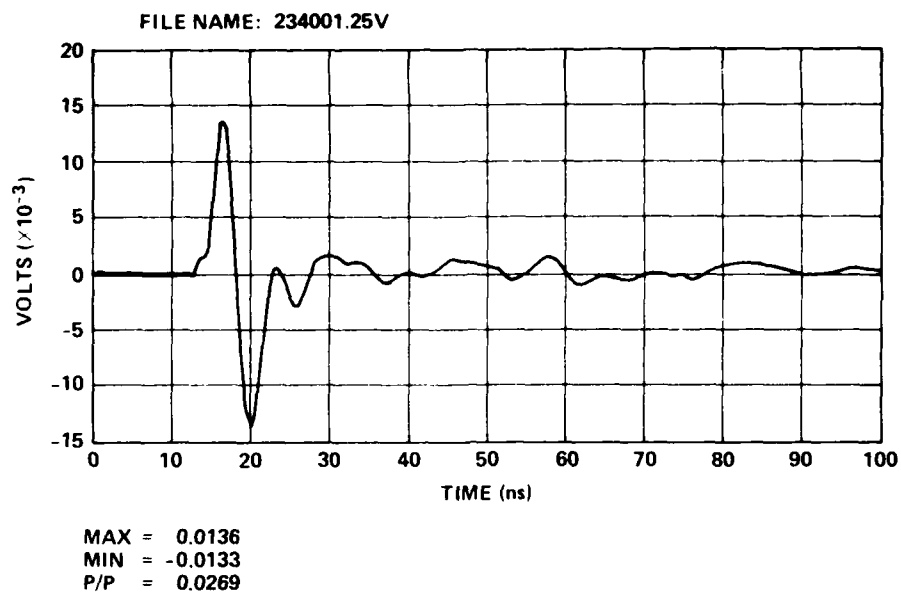


Figure 59. Configuration 9 vertical polarization experiment, test point 1, antenna mast group attached but not grounded: azimuth angle = 234 deg (file name does not reflect correct configuration).

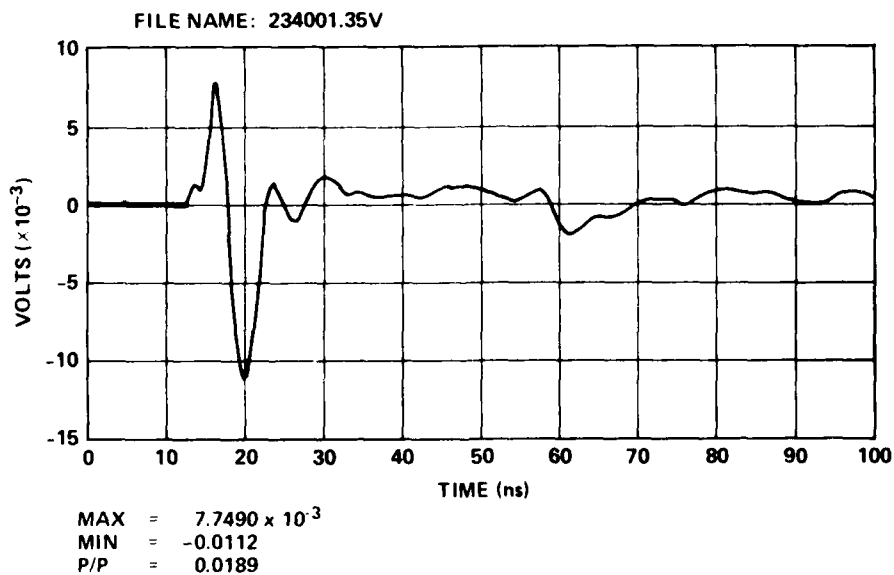


Figure 60. Configuration 9 vertical polarization experiment, test point 1, antenna mast group attached and grounded: azimuth angle = 234 deg (file name does not reflect correct configuration).

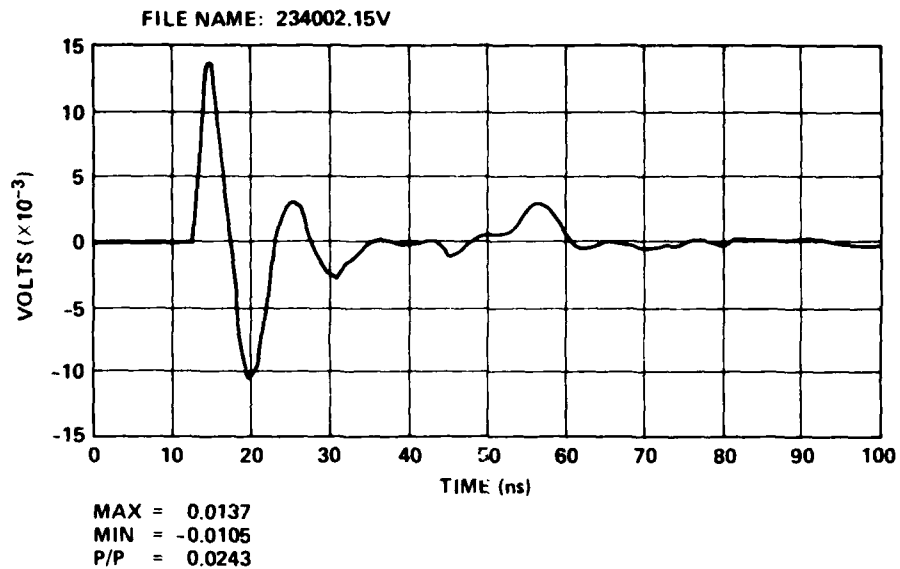


Figure 61. Configuration 9 vertical polarization experiment, test point 2, three vehicles, no antenna mast group: azimuth angle = 234 deg (file name does not reflect correct configuration).

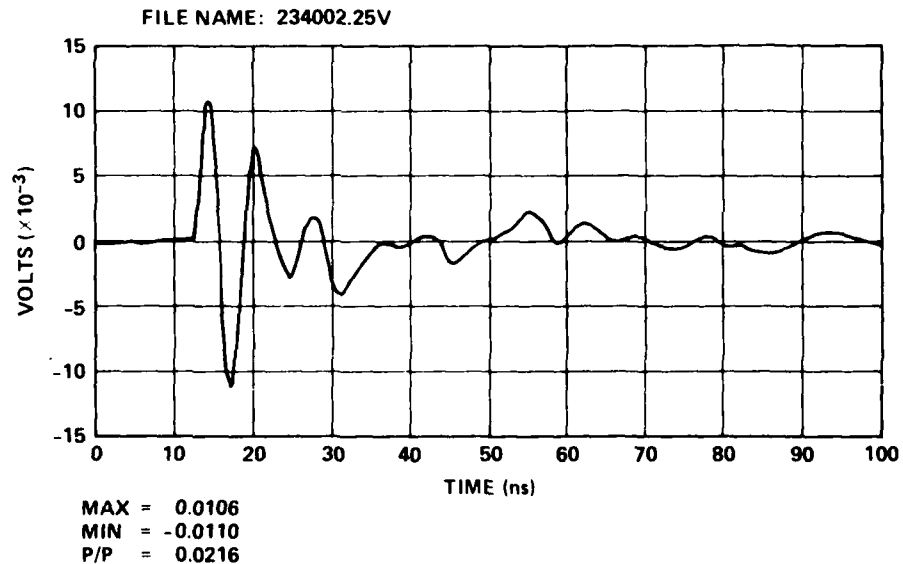


Figure 62. Configuration 9 vertical polarization experiment, test point 2, antenna mast group attached but not grounded: azimuth angle = 234 deg (file name does not reflect correction configuration).

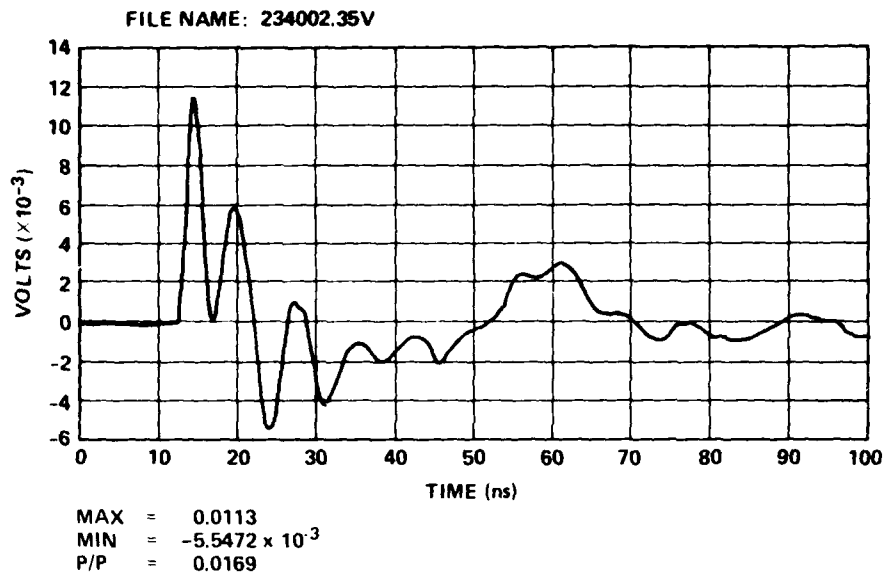


Figure 63. Configuration 9 vertical polarization experiment, test point 2, antenna mast group attached and grounded: azimuth angle = 234 deg (file name does not reflect correct configuration).

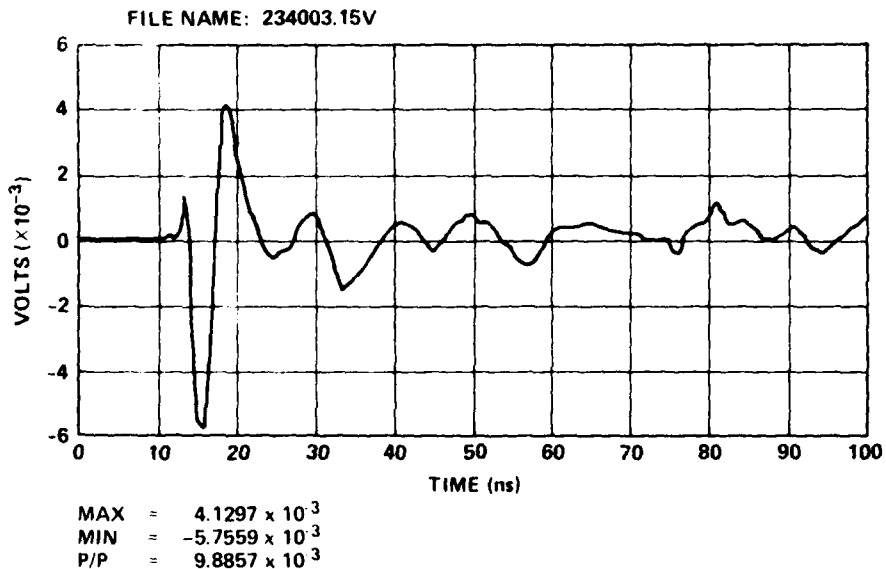


Figure 64. Configuration 9 vertical polarization experiment, test point 3, three vehicles, no antenna mast group: azimuth angle = 234 deg (file name does not reflect correct configuration).

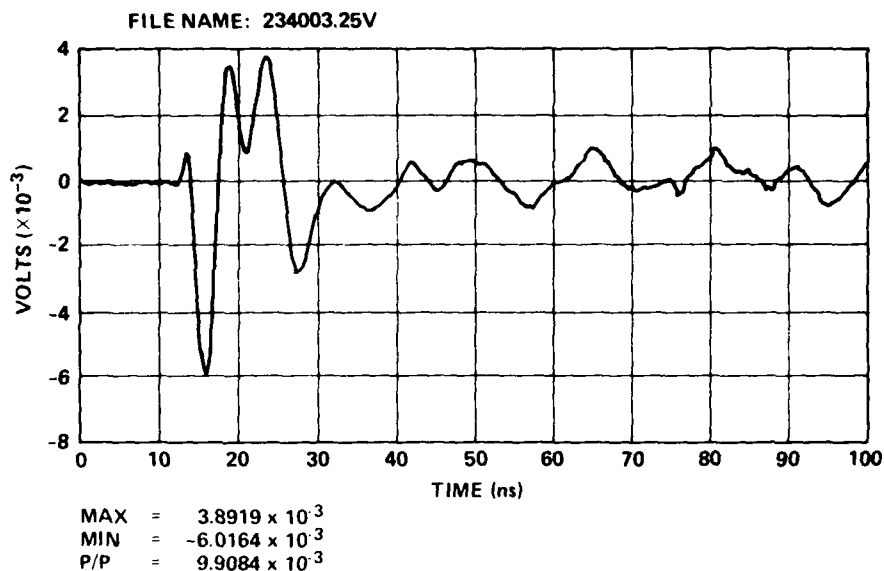


Figure 65. Configuration 9 vertical polarization experiment, test point 3, antenna mast group attached but not grounded: azimuth angle = 234 deg (file name does not reflect correct configuration).

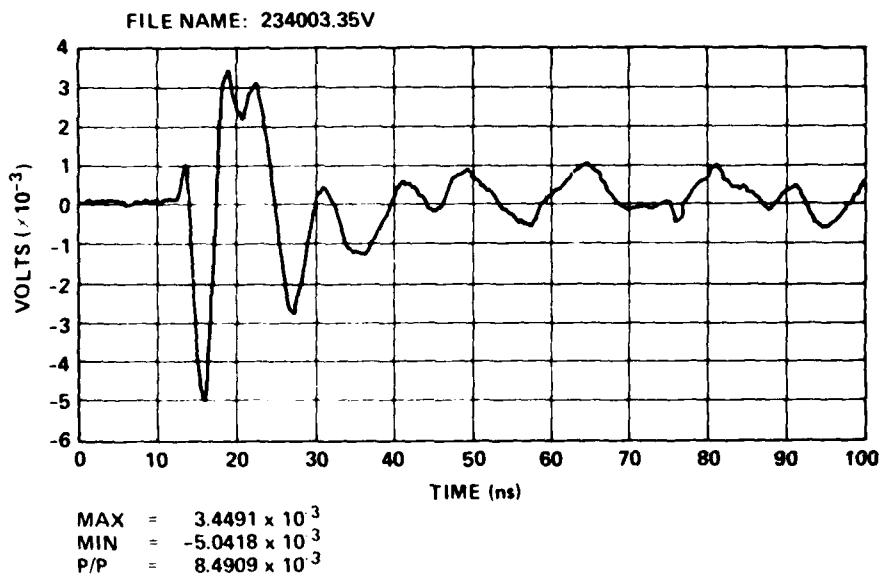


Figure 66. Configuration 9 vertical polarization experiment, test point 3, antenna mast group attached and grounded: azimuth angle = 234 deg (file name does not reflect correct configuration).

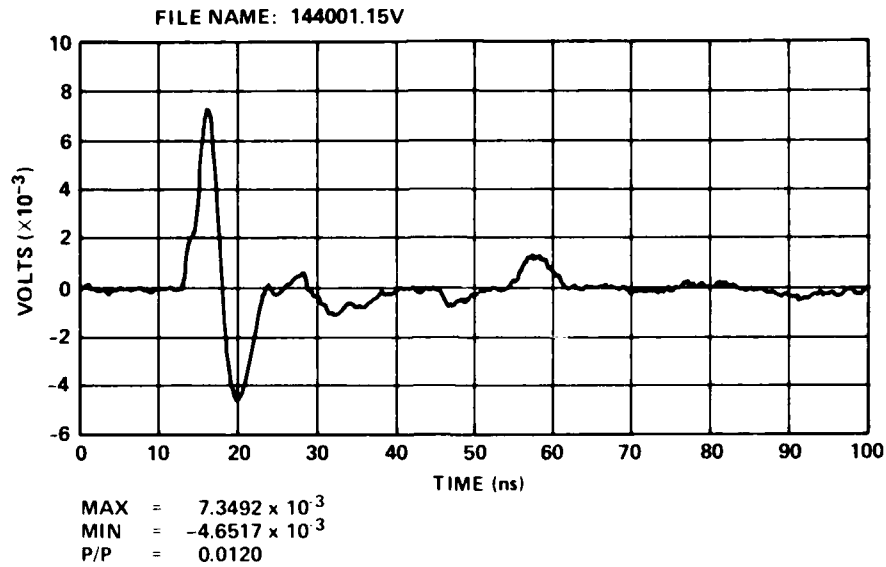


Figure 67. Configuration 9 vertical polarization experiment, test point 1, three vehicles grounded, no antenna mast group: azimuth angle = 144 deg (file name does not reflect correct configuration).

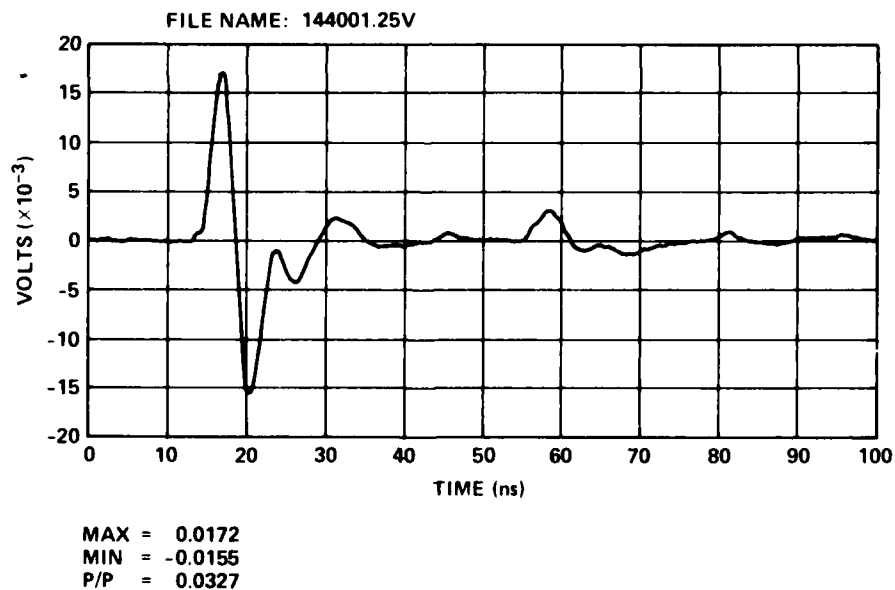


Figure 68. Configuration 9 vertical polarization experiment, test point 1, antenna mast group in place but not grounded: azimuth angle = 144 deg (file name does not reflect correct configuration).

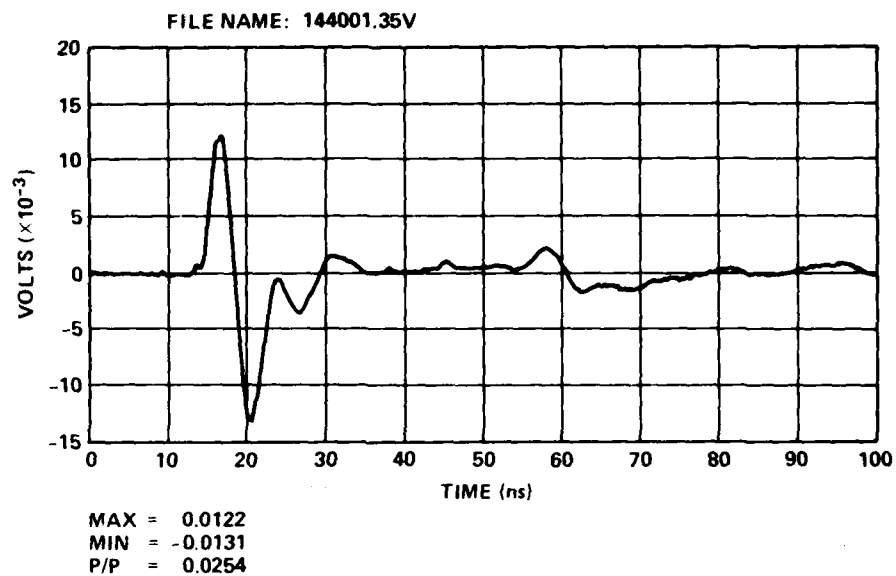


Figure 69. Configuration 9 vertical polarization experiment, test point 1, antenna mast group in place and grounded: azimuth angle = 144 deg (file name does not reflect correct configuration).

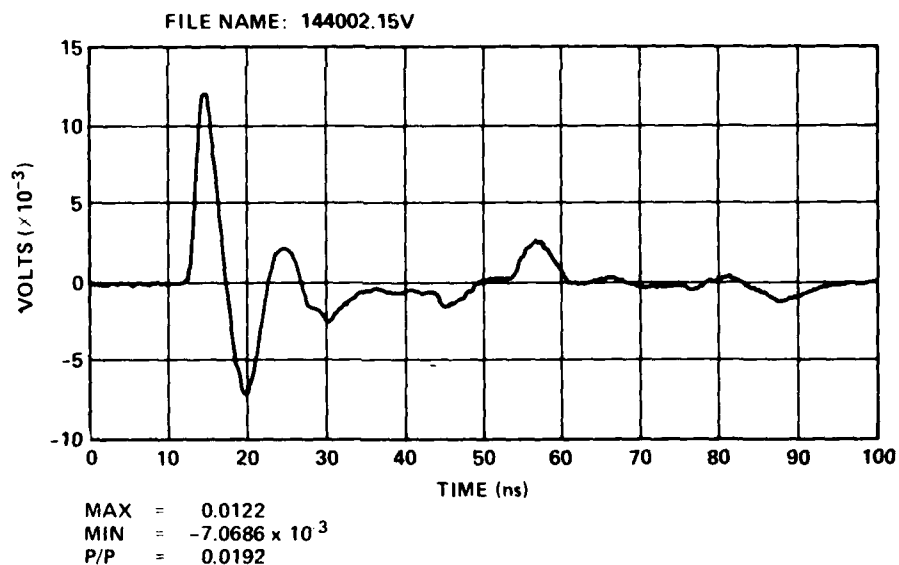


Figure 70. Configuration 9 vertical polarization experiment, test point 2, three vehicles each grounded, no antenna mast group: azimuth angle = 144 deg (file name does not reflect correct configuration).

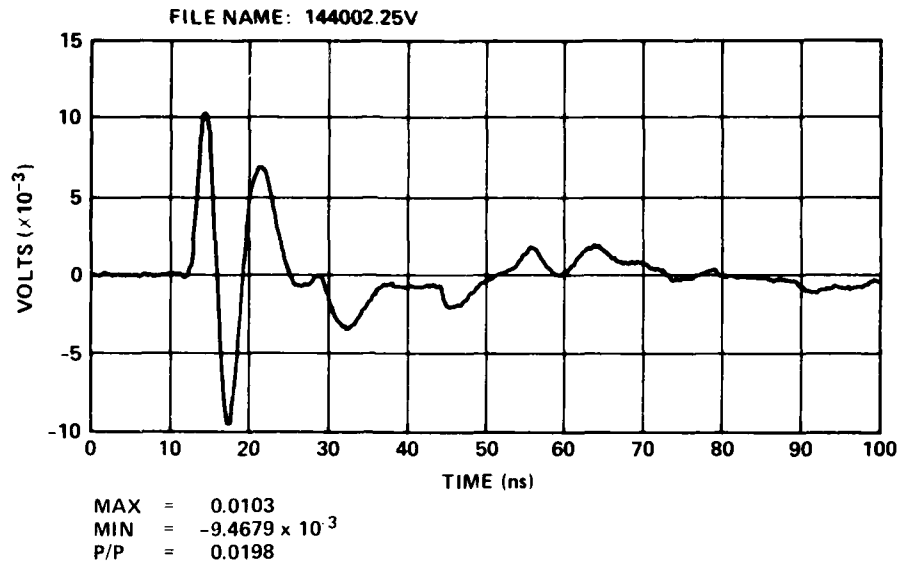


Figure 71. Configuration 9 vertical polarization experiment, test point 2, antenna mast group in place but not grounded: azimuth angle = 144 deg (file name does not reflect correct configuration).

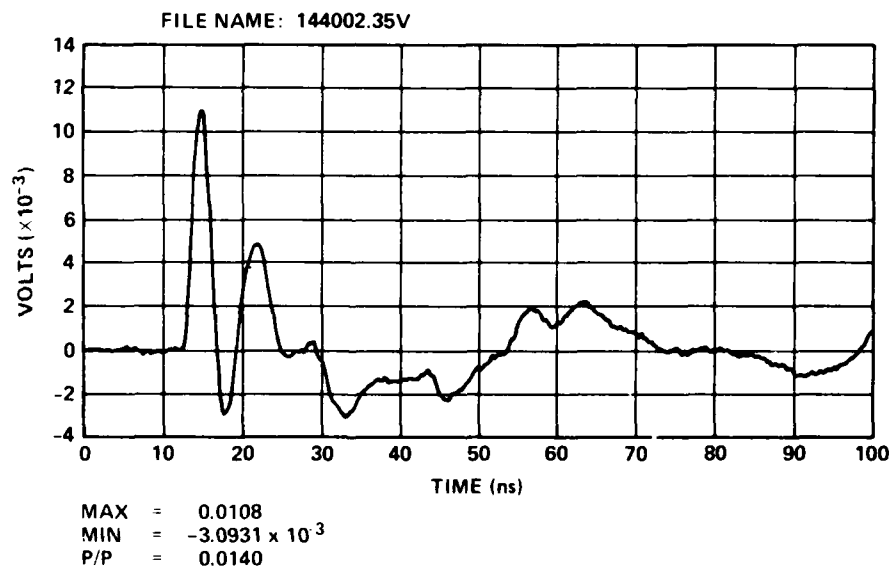


Figure 72. Configuration 9 vertical polarization experiment, test point 2, antenna mast group in place and grounded: azimuth angle = 144 deg (file name does not reflect correct configuration).

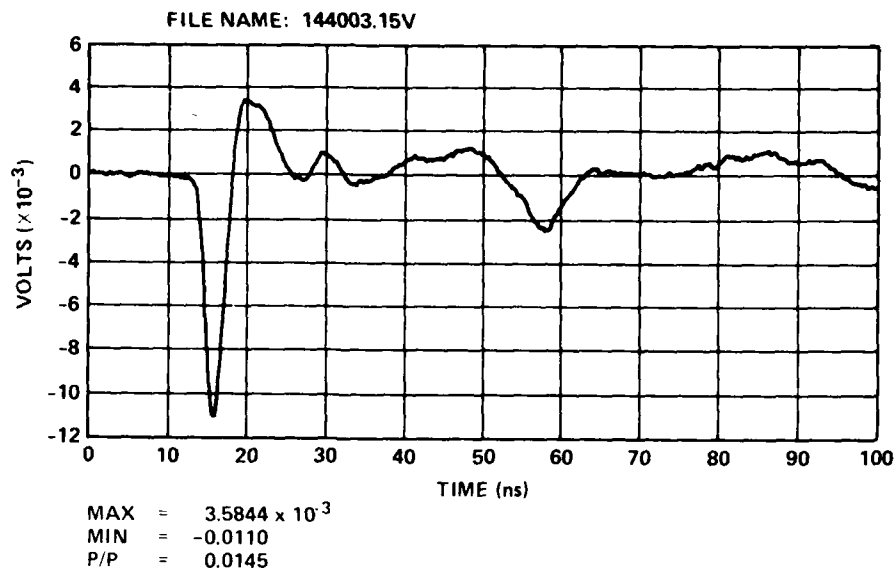


Figure 73. Configuration 9 vertical polarization experiment, test point 3, three vehicles each grounded, no antenna mast group: azimuth angle = 144 deg (file name does not reflect correct configuration).

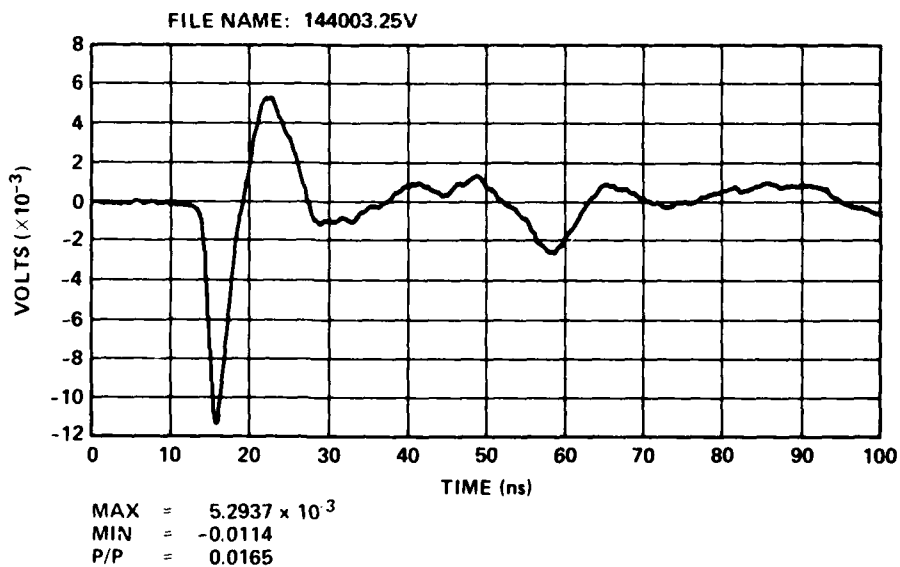


Figure 74. Configuration 9 vertical polarization experiment, test point 3, antenna mast group in place but not grounded: azimuth angle = 144 deg (file name does not reflect correct configuration).

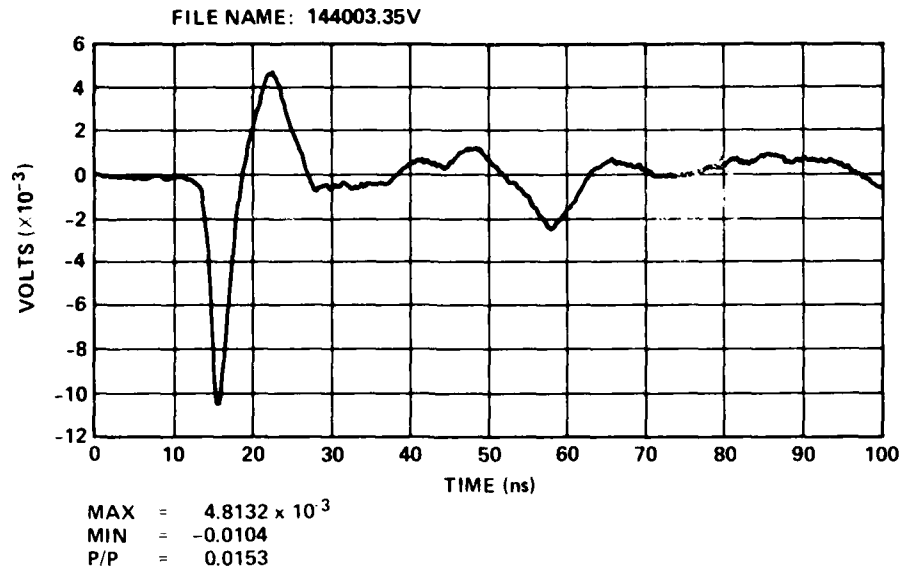
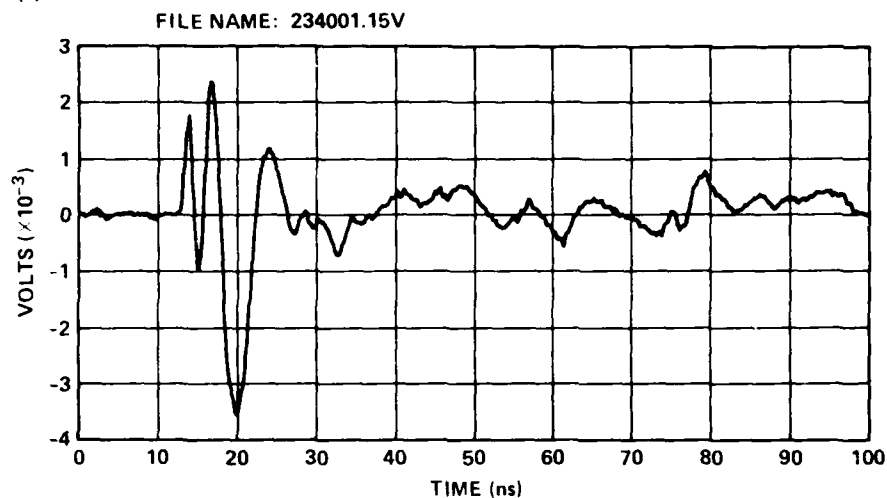


Figure 75. Configuration 9 vertical polarization experiment, test point 3, antenna mast group in place and grounded: azimuth angle = 144 deg (file name does not reflect correct configuration).

TABLE 6. RESPONSE OF PATRIOT MODEL TO VERTICAL ILLUMINATION

Test point	Azimuthal angle (deg)	Amplitude peak to peak (mV)		
		No antenna mast group (AMG)	AMG in place but not grounded	AMG grounded
1: Engagement control station	234	6.0	27.0	19.0
	144	12.0	32.5	25.5
2: Radar set	234	24.0	21.5	17.0
	144	19.5	20.0	14.0
3: Electric power plant	234	10.0	10.0	8.5
	144	14.5	16.5	15.5

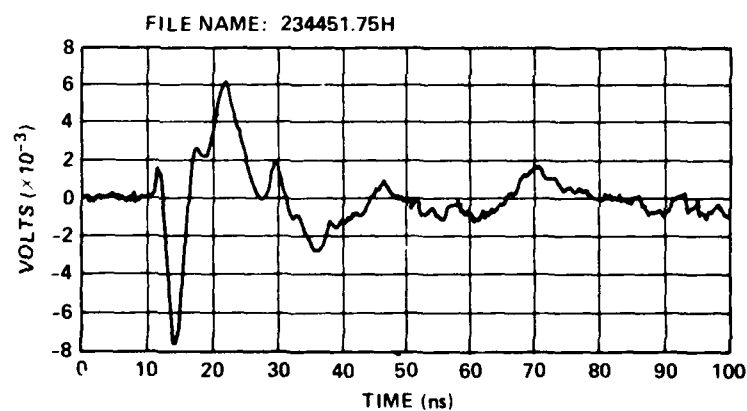
(a)



3 VEHICLES, NO AMG

MAX = 2.4234×10^{-3}
MIN = -3.5599×10^{-3}
P/P = 5.9834×10^{-3}

(b)



MAX = 8.3320×10^{-3}
MIN = -5.5722×10^{-3}
P/P = 0.0139

Figure 76. Configuration 9 test point 1, azimuth angle = 234 deg:
(a) vertical polarization experiment and (b) horizontal
polarization experiment, elevation angle = 45 deg (file names do
not reflect correct configuration).

5. SCALING UP DATA BY USING SCALING LAWS WITH ASSOCIATED PROBLEMS

5.1 General Considerations

According to the modeling theory (sect. 3), to transform the model data to the real world, the time scale in all model waveform time domain plots must be multiplied by the factor $p = 50$. In all model frequency domain plots, the frequency scale must be divided by the factor $p = 50$.

As pointed out in section 4.2, the model histograms and time domain plots can be converted to milliamperes by multiplying the amplitude by the factor 0.8 mA/mV. The model current amplitude is scaled to the real world current amplitude by using the formula

$$I = \frac{E}{E'}, (p)I' = \alpha pI' ,$$

where

I = current amplitude in real world,
 E = incident electric field in real world,
 E' = incident electric field in model world,
 $p = 50$,
 I' = current amplitude in model,
 α = scale factor for electric field intensity.

The derivation of the above equation assumes that the following relationships (sect. 3.1) are established for all the media being modeled:

$$\begin{aligned}\mu' &= \mu, \\ \epsilon' &= \epsilon, \\ \sigma' &= p\sigma.\end{aligned}$$

In practice, one can assume that $\mu' = \mu$, unless magnetic materials are used. The problem then is to properly scale the permittivity and the conductivity.

5.2 Scaling Permittivity and Conductivity

To investigate the problems associated with scaling model results up to real world expectations, an experiment was conducted in front of the Repetitive Electromagnetic Pulse Simulator (REPS), a horizontally polarized simulator, at the HDL Woodbridge, VA, Research Facility and a scale model version of the same experiment was conducted at the scale modeling facility. The experiment is detailed in section 5.3.

The dielectric constant (relative permittivity) and the conductivity of the REPS soil and the model soil were measured for HDL by the National Bureau of Standards, Boulder, CO. The results of these measurements are given in tables 7 to 9. Table 10 allows direct comparisons of actual model parameter values to ideally scaled REPS values for real world frequencies 1 and 50 MHz (assuming a scale factor of $p = 50$).

TABLE 7. DIELECTRIC CONSTANT AND CONDUCTIVITY OF REPS SOIL (SURFACE)

Frequency (MHz)	Received moisture content (%)	Dielectric constant	Conductivity (mmho/cm)	$\sigma/\omega\epsilon^*$
0.50	7.39	15.9	0.0065	1.47
0.75	7.39	13.3	0.0079	1.42
1.00	7.39	12.4	0.0090	1.31
50.0	7.39	6.15	0.0420	0.246
100.0	7.39	5.77	0.0542	0.169
150.0	7.39	5.55	0.0632	0.137

* σ = conductivity.
 ω = radian frequency.
 ϵ = permittivity.

TABLE 8. DIELECTRIC CONSTANT AND CONDUCTIVITY OF REPS SOIL (6-IN. DEPTH)

Frequency (MHz)	Received moisture content (%)	Dielectric constant	Conductivity (mmho/cm)	$\sigma/\omega\epsilon^*$
0.50	5.19	18.5	0.0066	1.28
0.75	5.19	15.7	0.0079	1.21
1.00	5.19	13.8	0.0091	1.19
50.0	5.19	5.68	0.0499	0.316
100.0	5.19	5.20	0.0668	0.231
150.0	5.19	4.95	0.0800	0.194

* σ = conductivity.
 ω = radian frequency.
 ϵ = permittivity.

TABLE 9. DIELECTRIC CONSTANT AND CONDUCTIVITY OF MODEL SOIL
(RANGE OF VALUES OBTAINED FROM THREE SAMPLES)

Frequency (MHz)	Received moisture content (%)	Dielectric constant	Conductivity (mmho/cm)	$\sigma/\omega\epsilon^*$
50.0	1 to 2	4.31 to 5.56	0.228 to 0.422	3.50 to 1.48
300.0	1 to 2	3.08 to 4.18	0.255 to 0.550	1.10 to 0.366
600.0	1 to 2	2.83 to 3.80	0.299 to 0.653	0.690 to 0.236
1200.0	1 to 2	2.67 to 3.58	0.390 to 0.847	0.467 to 0.219
2500.0	1 to 2	2.52 to 3.31	0.491 to 0.981	0.280 to 0.107
4000.0	1 to 2	2.51 to 3.24	0.576 to 1.51	0.270 to 0.080

* σ = conductivity.
 ω = radian frequency.
 ϵ = permittivity.

TABLE 10. ACTUAL MODEL PARAMETER VALUES AND SCALED REPS VALUES

Real world frequency (MHz)	Model frequency (MHz)	Dielectric constant scaled from REPS values*	Actual model† dielectric constant	Conductivity scaled from REPS values* (mmho/cm)	Actual model† conductivity (mmho/cm)
1.0	50.0	12.4 to 13.8	4.31 to 5.56	0.450 to 0.455	0.228 to 0.422
50.0	2500.0	5.68 to 6.15	2.52 to 3.31	2.10 to 2.50	0.491 to 0.981

*Depth range ~0 to 6 in.

†Depth range ~0 to 2 in.

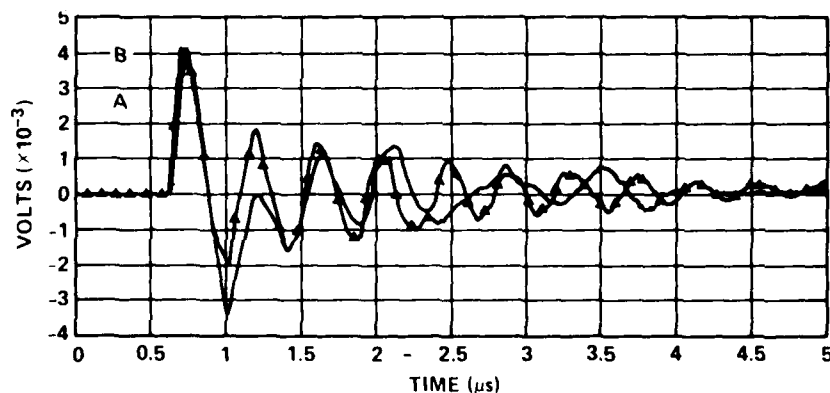
5.3 Coupling to Cable on and Above Ground in Real World and Model

A 61-m cable (RG 218) was laid in front of and parallel to the REPS at a ground range of 100 m. Its height aboveground was varied from 0 to 1.83 m. The external current in the center of the cable was monitored. The same experiment was performed at the scale modeling facility with the appropriate 1/50 scaling of wire length, range, height aboveground of the wire, and height aboveground of the antenna. The cable, which has a braided outer conductor, was modeled by a solid enamel coated wire. Actually, three wire gauges (No. 16, 26, and 36) were used for comparison. The results of the experiment are shown in

table 11, where the model data have been scaled up for comparison with the REPS data by using the formula in section 5.1. The REPS and model waveforms can be compared in figures 77 to 79. The peak amplitudes have been set equal.

TABLE 11. PEAK TO PEAK CURRENT ON WIRE IN MODEL AND IN FRONT OF REPS

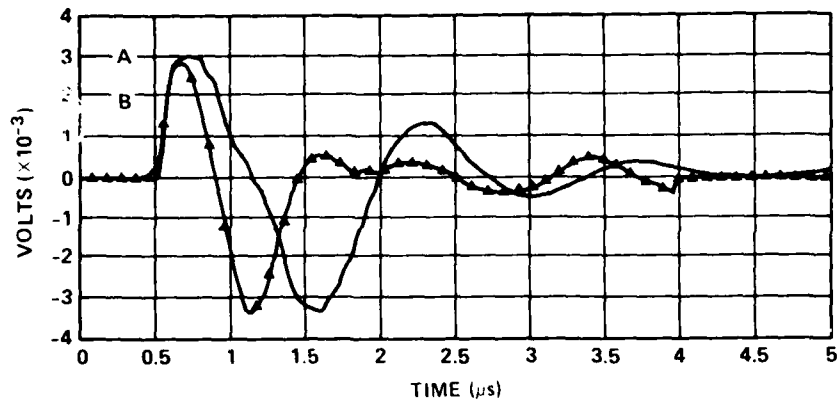
Experiment	Current peak to peak (A)		
	Conductor on ground	Conductor 0.91 m (1.82 cm) aboveground	Conductor 1.83 m (3.64 cm) aboveground
REPS	7.0	5.0	6.5
Model			
No. 16 wire	36.5	22.7	24.3
No. 26 wire	28.7	19.4	20.5
No. 36 wire	16.6	15.5	15.5



WAVEFORM A 4 FT WIRE AWG 36 1-7/16 IN., FILE NAME: JUNE21.14

WAVEFORM B (TRIANGLES), FILE NAME: JUNE21.14D

Figure 77. Wire aboveground: waveform A = model data and waveform B = field data.



WAVEFORM A, FILE NAME: JUNE21.19D

WAVEFORM B 4 FT WIRE AWG 26 (TRIANGLES), FILE NAME: JUNE21.11

Figure 78. Wire on ground: waveform A = field data and waveform B = model data.

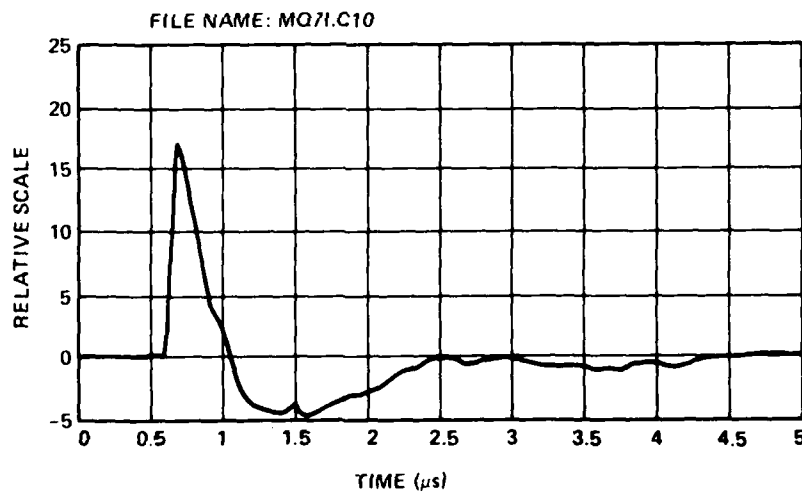


Figure 79. Horizontally polarized model incident field, magnetic field measurement (time has been scaled up).

As the outer diameter of the model wire becomes smaller (No. 16 wire is largest and No. 36 wire is smallest), the agreement with the REPS experiment improves. This improvement encourages one to want to justify using as small a wire as necessary, if practical to achieve agreement. Ideally, to empirically determine what size of wire is required, using the experimental current data, one must address the whole problem and either exactly model the ground parameters permittivity (ϵ) and conductivity (σ) or account for how errors in the model ground parameters propagate to cause an error in the current in a wire of arbitrary diameter. This is a formidable problem as the wire approaches the ground. A very accurate mathematical model is needed that describes the interaction of the total field near a boundary, having a complex permittivity, with a conductor on or near its surface. The existing computer code used in HDL is not equipped to relate variations in the complex permittivity to variations in the conductor current.

Consequently, the task of modeling the coupling to a cable near the ground breaks down into two specific and distinct areas: reducing errors associated with modeling the ground and reducing errors associated with modeling the cable. Unfortunately, when viewed from the point of view of analyzing experimental data (current on the wire in the model), the effects of these two types of errors cannot be separated.

Below we outline some theoretical considerations associated with coupling to a wire connecting two vehicles in the model.

Assume that the real world cable can be considered as a thin walled tubular outer conductor with a center conductor inside. If, for example, the ratio of wall thickness (d) to skin depth (δ) is 0.5, then⁴

$$\frac{R}{R_{hf}} = 2$$

and

$$\frac{\omega L_i}{R_{hf}} = 0.25$$

where the surface impedance (Z^{tube}) per square is

$$Z^{\text{tube}} = R + j\omega L_i$$

⁴Simon Ramo, John Whinnery, and Theo. Van Duzer, *Fields and Waves in Communications Electronics*, John Wiley & Sons, Inc., New York (1965), 302.

and

R = resistance per unit length,
 $R_{hf} = R_s / 2\pi r_o$ = high frequency resistance per unit length,
 R_s = surface resistivity,
 r_o = radius to outer surface,
 ω = radian frequency,
 L_i = internal inductance per unit length.

Therefore, we have

$$\begin{aligned}
 Z^{\text{tube}} &= 2R_{hf} + j(0.25)R_{hf} \\
 &= \frac{2R_s}{2\pi r_o} + j \frac{(0.25)R_s}{2\pi r_o} \\
 &= \frac{R_s}{2\pi r_{\text{eff}}} + j \frac{(0.125)R_s}{2\pi r_{\text{eff}}} .
 \end{aligned}$$

Thus, we can think of the tube as being replaced with a solid cylindrical conductor of surface resistivity R_s , having a radius equal to r_{eff} , where r_{eff} is the effective radius of the tube, which is much greater than skin depth,

$$r_{\text{eff}} = \frac{r_o}{2} .$$

We can write in general, for $d/\delta < 0.5$, since the inductive part of the surface impedance is small compared with the resistive part,

$$Z^{\text{tube}} \approx \frac{R_s}{2\pi r_{\text{eff}}} ,$$

where r_{eff} is some fraction of the physical radius. We have assumed here that the external inductance of the conductor is small and have not considered it; of course, this is not true in general. Now let us transform this formula to the domain of the model. The scaling formulas used are

$$f' = p_1 f \quad ,$$

$$\sigma' = p_2 \sigma \quad ,$$

$$l' = l/p_3 \quad ,$$

where the primed macroscopic quantities refer to the model and the unprimed quantities refer to the full-scale system and

f = frequency,

σ = conductivity,

l = physical length,

p = scale factor.

The wire that models the thin walled tubular outer conductor has an impedance per unit length

$$\begin{aligned} Z^{\text{tube}'} &= \frac{R'_s}{2\pi r'_{\text{eff}}} \\ &= \frac{\left(\frac{\pi p_1 t \mu}{p_2 \sigma} \right)^{1/2}}{\frac{2\pi r_{\text{eff}}}{p_3}} \\ &= \left(\frac{p_1}{p_2} \right)^{1/2} p_3 \left(\frac{R_s}{2\pi r_{\text{eff}}} \right) . \end{aligned}$$

If we view two model vehicles such as the ECS and the RS, connected together by a wire as a circuit (wavelength very long compared with physical length), where the inductance and the resistance are associated with the wire and the capacitance to ground is associated with the

vehicles, then at resonance the impedance (resistance) of the model circuit wire is given by the expression $Z^{\text{tube}}_{\ell'}$. The current in the circuit is given by

$$I' = \frac{v'}{Z^{\text{tube}}_{\ell'} + Z'\ell'}$$

where v' is an equivalent source⁵ due to the incident and scattered field components at the wire, Z' is the impedance due to ground losses in the model, and ℓ' is the wire length. Substituting the expression for $Z^{\text{tube}}_{\ell'}$ and eliminating the primes from the right-hand side of the equation (except for Z') yield

$$\begin{aligned} I' &= \frac{\frac{v}{\alpha p_3}}{\left(\frac{p_1}{p_2}\right)^{1/2} p_3 \left(\frac{R_s \ell / p_3}{2\pi r_{\text{eff}}} \right) + \frac{Z' \ell}{p_3}} \\ &= \frac{v}{\alpha p_3 \left[\left(\frac{p_1}{p_2}\right)^{1/2} \frac{R_s \ell}{2\pi r_{\text{eff}}} + \frac{Z' \ell}{p_3} \right]} \end{aligned}$$

Using the following values for the scaling parameters appropriate for the PATRIOT effort, $p_1 = p_3 \approx 50$ and $p_2 = 1$, we obtain

$$I' = \frac{v}{50\alpha \left(\sqrt{50} \frac{R_s \ell}{2\pi r_{\text{eff}}} + \frac{Z' \ell}{50} \right)}$$

where α is the scale factor for electrical intensity as stated in section 3.1.

The following expression for Z' has been given by Kohlberg⁶ for the case where the height of the conductor aboveground to the skin depth in the ground is very large:

⁵K. Lee, Two Parallel Terminated Conductors in External Fields, IEEE Trans. Electromag. Compat., EMC-20 (May 1978).

⁶I. Kohlberg, A Theoretical Study of the TEMPS Simulator, XRI Corp. Contract with Harry Diamond Laboratories DAAG39-76-C-0166 (July 1977).

$$Z' = \frac{Z'_{in}}{2\pi h'} ,$$

where

Z'_{in} = intrinsic impedance of model earth,
 h' = height aboveground of wire in model ($h' = h/50$ for present case).

Assuming that ideal scaling exists, that is, $p_1 = p_2 = p_3 = 50$,
 then

$$\begin{aligned} I' &= \frac{V}{50\alpha \left[\frac{R_s \ell}{2\pi r_{eff}} + \frac{Z'_{in} (\ell/50)}{2\pi (h/50)} \right]} \\ &= \frac{V}{50\alpha \left(\frac{R_s \ell}{2\pi r_{eff}} + \frac{Z'_{in} \ell}{2\pi h} \right)} . \end{aligned}$$

If the conductivity and the dielectric constant of the model are scaled properly, then $Z'_{in} = Z_{in}$, where Z_{in} is the intrinsic impedance of the real world ground, yielding

$$I' = \frac{V}{50\alpha \left(\frac{R_s \ell}{2\pi r_{eff}} + \frac{Z_{in} \ell}{2\pi h} \right)} ;$$

hence,

$$I' = \frac{I}{50\alpha} .$$

6. CONCLUSIONS

a. Maximum coupling to a reasonably straight cable between two vehicles is broadside in the azimuthal plane for horizontal polarization.

b. Coupling to the straight cable increases as the angle of elevation (measured with respect to the ground) increases. Maximum coupling occurs when the source is overhead.

c. A review of the data shows that the currents excited by vertically as well as horizontally polarized fields can be significant and should be considered in analyzing the coupling to the PATRIOT system.

d. Grounding the AMG is probably a good idea for EMP protection. However, grounding the other vehicles is probably not critical for EMP protection.

e. There is evidence that, for a loose Y configuration (1), the individual legs of the system behave approximately as though the other legs were absent.

f. The model system seems to be responding as a circuit (resonant wavelength much greater than physical length) with the capacitance provided by the interaction of the vehicles with ground and the inductance and the resistance provided by the wire.

g. The Δ configuration probably will couple larger currents to the system than the Y configuration.

h. A tight Y configuration (6) seems to couple more to the incident field than a loose Y configuration (1) with shorter sides.

LITERATURE CITED

- (1) PATRIOT Air Defense System, Raytheon Co. Missile Systems Div., PATRIOT Program Office, Bedford, MA, Br. 10165, Rev. A (February 1978).
- (2) G. Sinclair, Theory of Models of Electromagnetic Systems, Proceedings of IRE (November 1948), 1364-1370.
- (3) Andrew A. Cuneo, Jr., and James J. Loftus, Measurement of Scaled Down High-Altitude Electromagnetic Pulse (HEMP) Waveforms, Harry Diamond Laboratories HDL-TM-81-6 (March 1981).
- (4) Simon Ramo, John Whinnery, and Theo. Van Duzer, Fields and Waves in Communications Electronics, John Wiley & Sons, Inc., New York (1965), 302.
- (5) K. Lee, Two Parallel Terminated Conductors in External Fields, IEEE Trans. Electromag. Compat., EMC-20 (May 1978).
- (6) I. Kohlberg, A Theoretical Study of the TEMPS Simulator, XRI Corp. Contract with Harry Diamond Laboratories DAAG39-76-C-0166 (July 1977).

APPENDIX A.--CALCULATION OF FIELDS FROM VERTICALLY AND HORIZONTALLY
POLARIZED RADIATORS FOR PATRIOT SYSTEM ILLUMINATION

PRECEDING PAGE BLANK-NOT FILMED

APPENDIX A

To act as a vertical radiator for the PATRIOT system, a resistively tapered vertical wire was connected directly to a General Radio connector mounted on an aluminum ground plane 6×6 ft (1.8×1.8 m). This wire was driven by the same pulse generator as used for the horizontally polarized dipole. A time domain reflectometry measurement of the vertical wire yielded a reflection coefficient (Γ) of 0.74 when the reflection was considered only from the feed point to the second resistor. The antenna impedance is calculated to be

$$\begin{aligned} Z_K &= Z_0 \frac{1 + \Gamma}{1 - \Gamma} \\ &= 50 \frac{(1 + 0.74)}{(1 - 0.74)} \\ &= 335 \text{ ohms} \end{aligned}$$

The voltage driving the feed point of the tapered vertical antenna is computed to be

$$\begin{aligned} V_0 &= V_{inc} (1 + \Gamma) \\ &= 840(1.74) \\ &= 1462 \text{ V} \end{aligned}$$

At a range of 3 m, the radiated vertically polarized electric field is calculated by the following formula:

$$E_{pk}^{inc} = \frac{60V_0}{rZ_K}$$

where

V_0 = driving voltage,
 r = radial distance,
 Z_K = antenna impedance

APPENDIX A

so that

$$\begin{aligned} E_{pk}^{inc} &= \frac{(60)(1462)}{(3)(335)} \\ &= 87 \text{ V/m} . \end{aligned}$$

The peak horizontally polarized electric field generated for this experiment was calculated by measuring the incident and reflected voltages associated with the model radiator. From this information, one computes the voltage driving the bicone. Using the above formula, one calculates the peak radiated electric field,

$$\begin{aligned} E_{pk}^{inc} &= \frac{(60)(1461 \text{ V})}{(3.1 \text{ m})(300 \text{ ohms})} \\ &= 94 \text{ V/m} . \end{aligned}$$

APPENDIX B.--EXPERIMENT OF PATRIOT SYSTEM TO STUDY COUPLING TO
COLLINEARLY ARRANGED ENGAGEMENT CONTROL STATION,
ANTENNA MAST GROUP, AND ELECTRIC POWER PLANT

CONTENTS

	<u>Page</u>
TEXT	85

FIGURES

B-1. Coupling to collinearly arranged engagement control station, antenna mast group and power plant	85
B-2. Response of wire with engagement control station present	86
B-3. Response of wire with engagement control station removed	86
B-4. Fast Fourier transforms of cable response with and without engagement control station	87

The purpose of this experiment on the PATRIOT system was to determine the effect of removing the engagement control station (ECS) on the current measured on the wire from the ECS to the electric power plant (EPP) near the location of the ECS. The configurations of the models and the radiator are shown in figure B-1. Figures B-2 and B-3 show the time domain waveforms for the configurations with and without the ECS, respectively. Figure B-4 compares the fast Fourier transforms of the two configurations.

The conclusion drawn here is that there is no significant difference between the two configurations. This conclusion renders the three collinearly arranged vehicle layout tractable for calculating cable current.

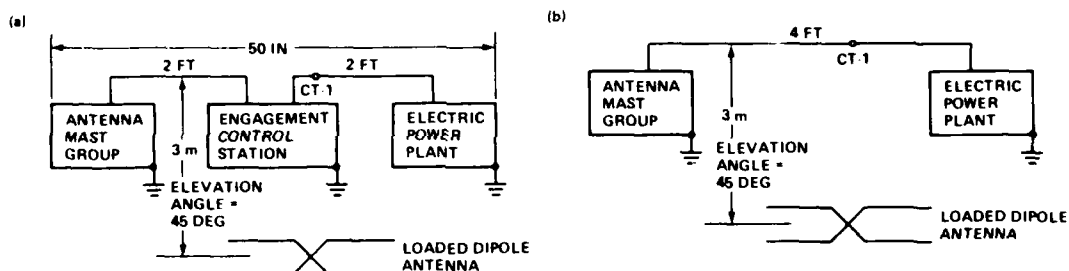


Figure B-1. Coupling to collinearly arranged engagement control station (ECS), antenna mast group, and power plant (a) with ECS and (b) without ECS.

APPENDIX B

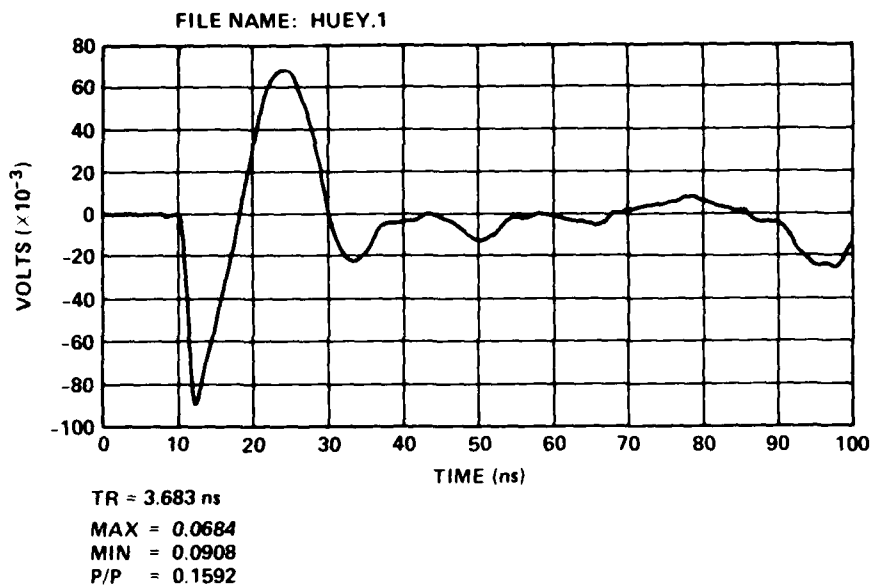


Figure B-2. Response of wire with engagement control station present.

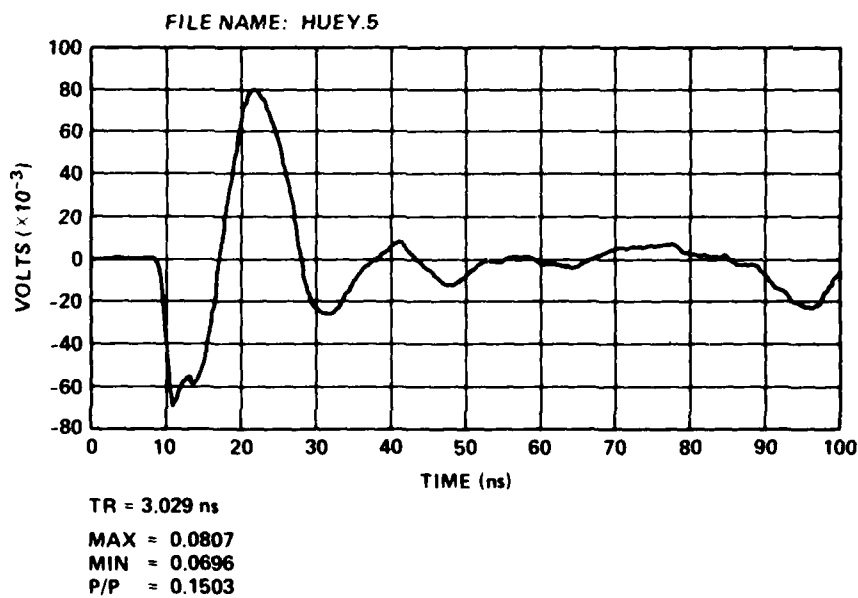
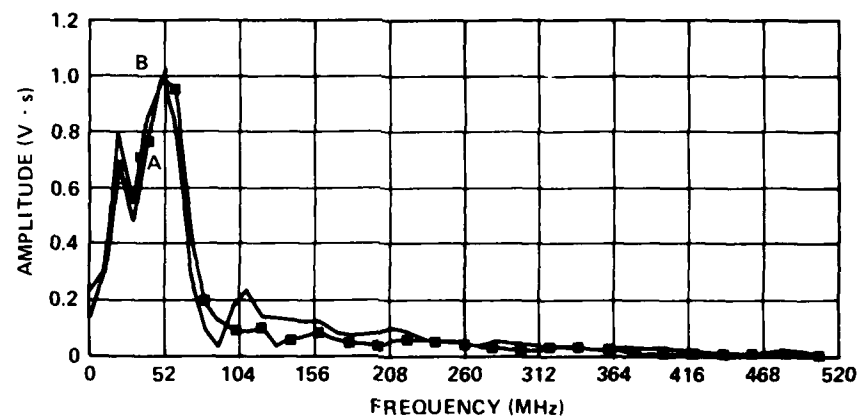


Figure B-3. Response of wire with engagement control station removed.

APPENDIX B



FFT A MAX(A) IS AT 5×10^7 Hz, FILE NAME: HUEY.1

FFT B MAX(B) IS AT 5×10^7 Hz, FILE NAME: HUEY.5

Figure B-4. Fast Fourier transforms of cable response with and without engagement control station.

APPENDIX C.--EXPERIMENT OF PATRIOT SYSTEM TO COMPARE THE RESPONSE OF
A MODEL WIRE ABOVEGROUND WITH HORIZONTALLY AND VERTICALLY
POLARIZED INCIDENT FIELDS

CONTENTS

	<u>Page</u>
TEXT	91
C-1. Broadside coupling to horizontally polarized field, time domain response	91
C-2. End-fire coupling to vertically polarized field, time domain response	92
C-3. Comparison of broadside horizontal and end-fire vertical coupling, time domain response	92
C-4. Comparison of broadside horizontal and end-fire vertical coupling, fast Fourier transforms	93
C-5. Broadside coupling to vertical field, time domain response ...	93
C-6. End-fire coupling to horizontal field, time domain response ...	94
C-7. Broadside and end-fire incident field orientations	94

APPENDIX C

We see from figures C-1 to C-6 that a horizontally polarized field will couple more strongly to a wire aboveground than a vertically polarized field for the orientations shown in figure C-7 for the PATRIOT system. It is assumed here that the incident fields are of the same amplitude. Indeed, they are very close in amplitude (sect. 3.5 in the main body of this report).

The dominant coupling mode for a horizontally polarized field is broadside, and that for a vertically polarized field is end fire.

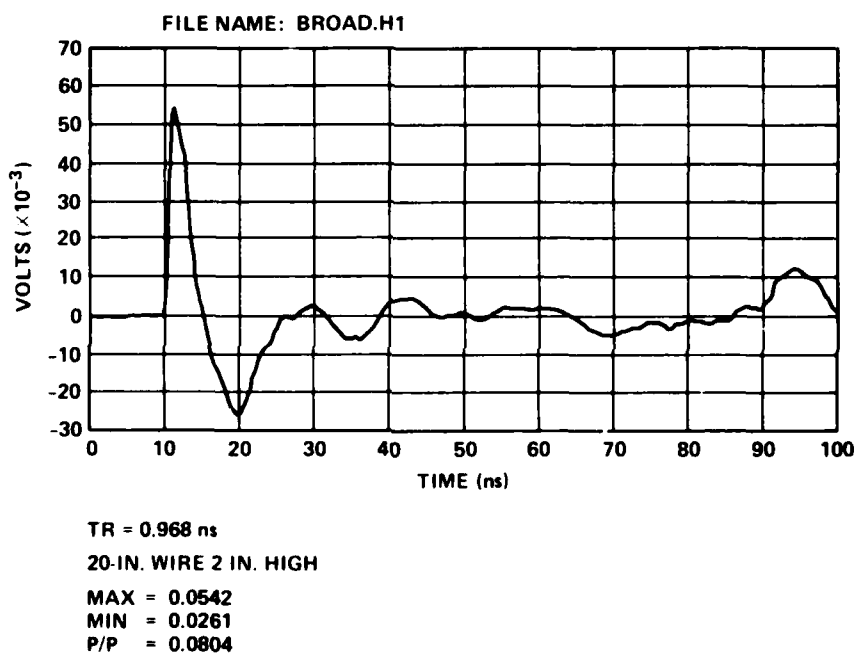


Figure C-1. Broadside coupling to horizontally polarized field, time domain response.

APPENDIX C

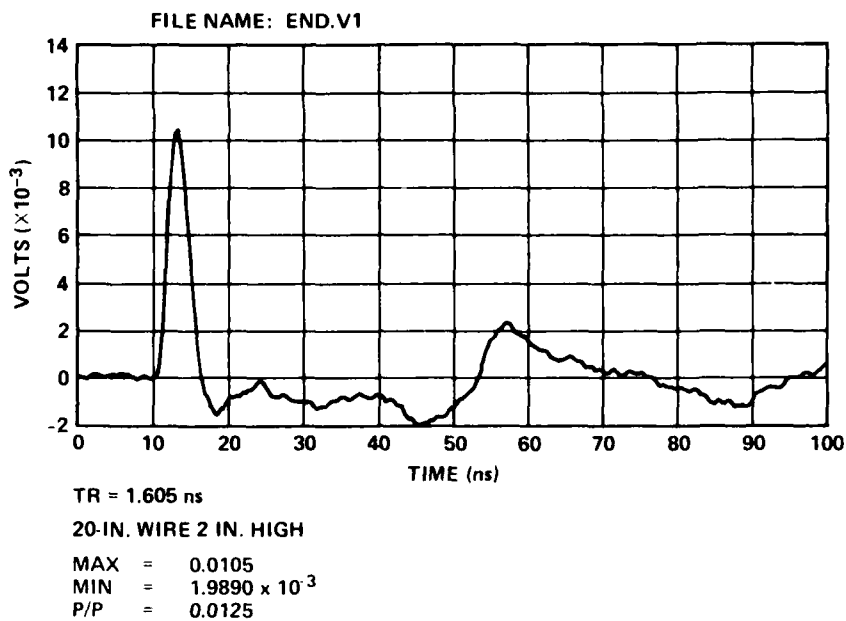


Figure C-2. End-fire coupling to vertically polarized field, time domain response.

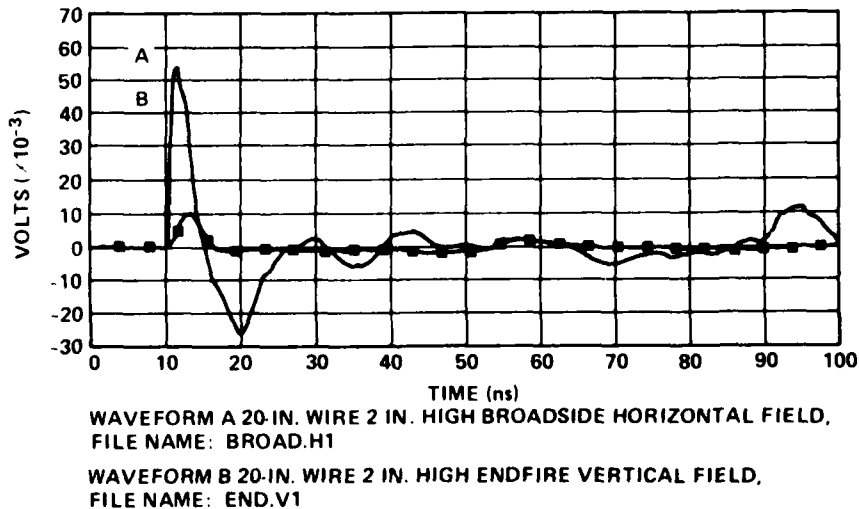
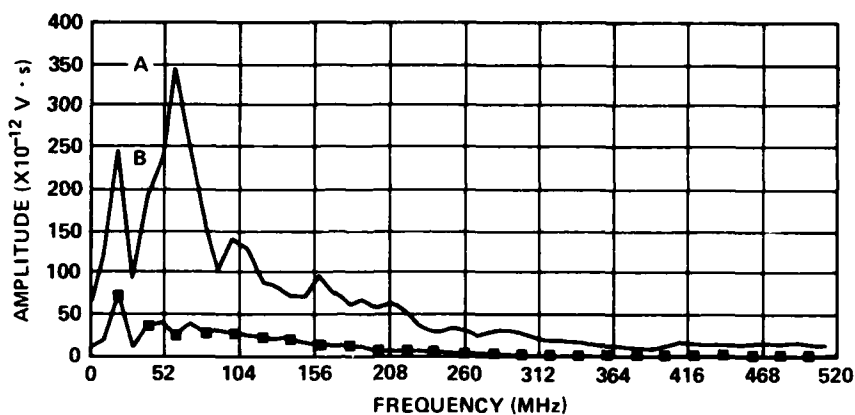


Figure C-3. Comparison of broadside horizontal and end-fire vertical coupling, time domain response.



FFT A 20-IN. WIRE 2 IN. HIGH BROADSIDE HORIZONTAL FIELD,
MAX(A) IS AT 6×10^7 Hz, FILE NAME: BROAD.H1

FFT B 20-IN. WIRE 2 IN. HIGH ENDFIRE VERTICAL FIELD,
MAX(B) IS AT 2×10^7 Hz, FILE NAME: END.V1

Figure C-4. Comparison of broadside horizontal and end-fire vertical coupling, fast Fourier transforms.

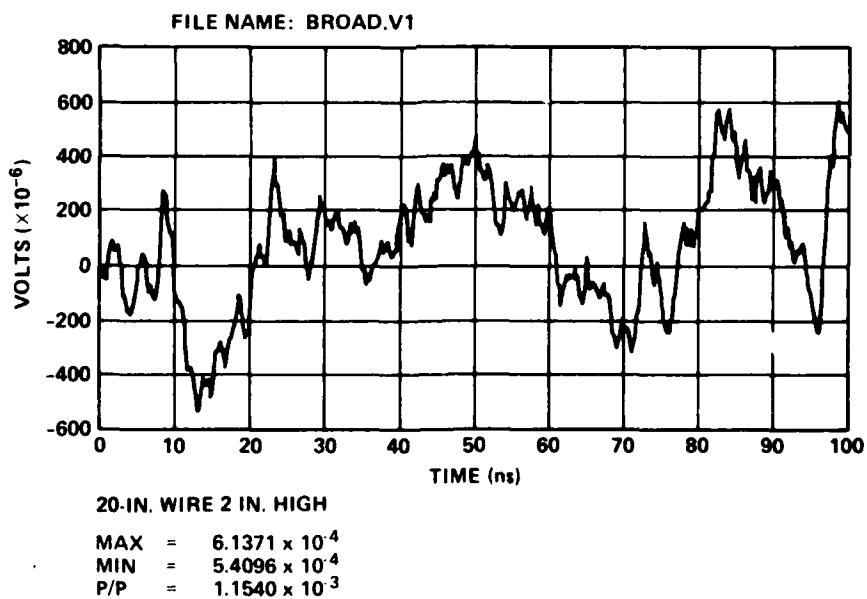


Figure C-5. Broadside coupling to vertical field, time domain response.

APPENDIX C

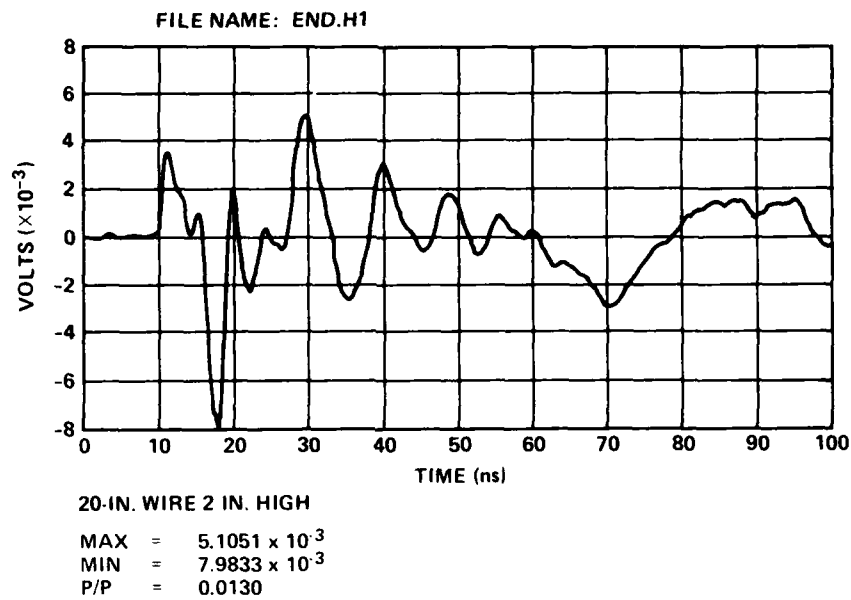


Figure C-6. End-fire coupling to horizontal field, time domain response.

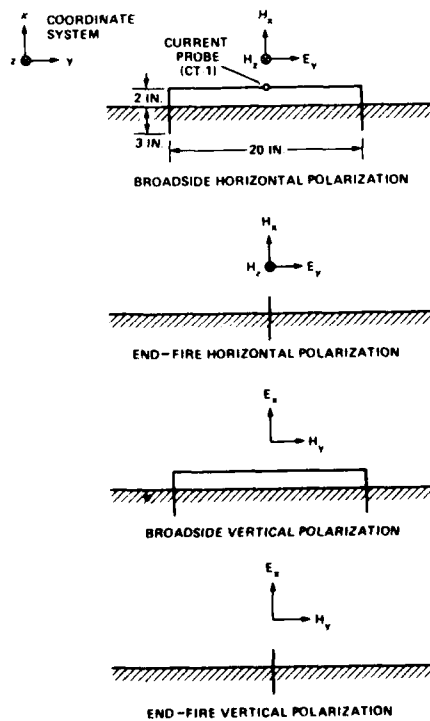


Figure C-7. Broadside and end-fire incident field orientations.

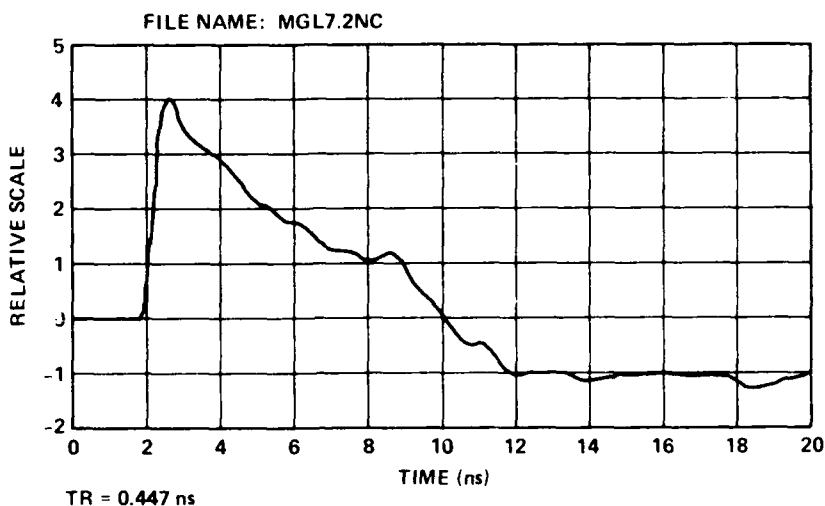
APPENDIX D.--RADIATED FIELD WAVEFORMS OF PATRIOT SYSTEM

CONTENTS

	<u>Page</u>
TEXT	97
D-1. Horizontally polarized incident field, magnetic field measurement	97
D-2. Vertically polarized incident field	98

Presented in figures D-1 and D-2 are the time domain representations of the radiated fields from the horizontally and vertically polarized radiators for the PATRIOT system. See section 3.5 in the main body of this report for the peak amplitudes of the radiated fields.

(a)



(b)

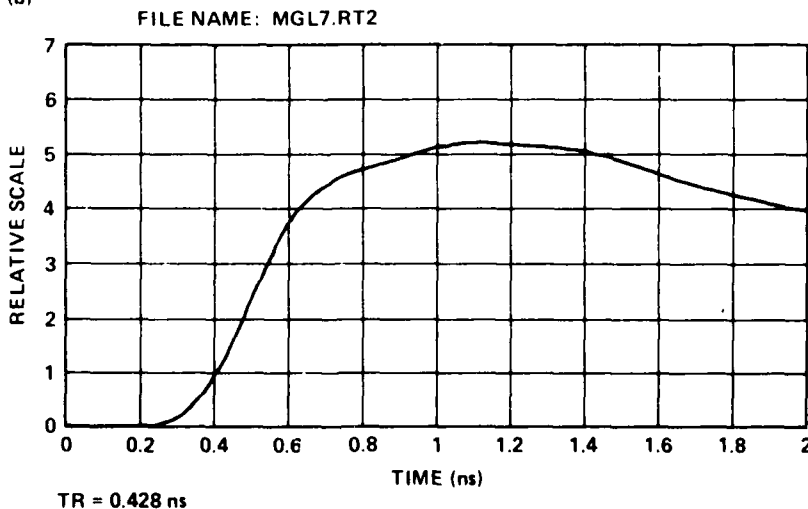


Figure D-1. Horizontally polarized incident field, magnetic field measurement.

AU-A107 480

HARRY DIAMOND LABS ADELPHI MD
SCALE MODELING FOR THE PATRIOT
MAY 81 A A CUNEO, J J LOFTUS

ELECTROMAGNETIC PULSE TEST.(U)

F/G 16/4.2

UNCLASSIFIED

HUL-TM-81-16

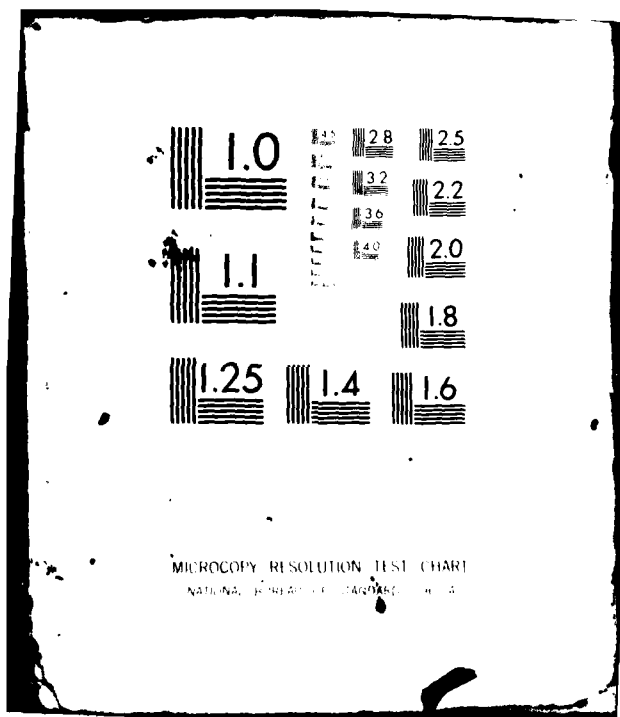
NL

2-12

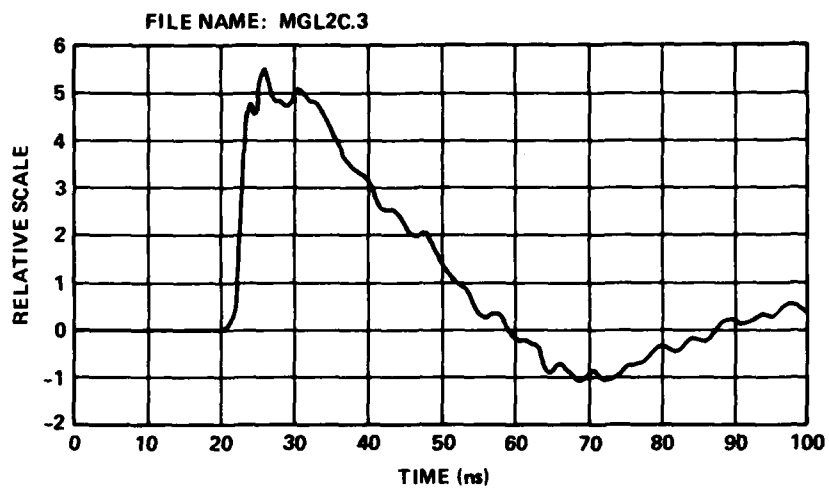
AD 1010



END
DATE
FILMED
12 81
DTIC



APPENDIX D



TR = 3.429 ns

Figure D-2. Vertically polarized incident field.

DISTRIBUTION

ADMINISTRATOR
DEFENSE TECHNICAL INFORMATION CENTER
CAMERON STATION, BUILDING 5
ATTN DTIC-DDA (12 COPIES)
ALEXANDRIA, VA 22314

COMMANDER
US ARMY RSCH & STD GP (EUR)
ATTN CHIEF, PHYSICS & MATH BRANCH
FPO NEW YORK 09510

COMMANDER
US ARMY ARMAMENT MATERIEL
READINESS COMMAND
ATTN DRSAR-LEP-L, TECHNICAL LIBRARY
ATTN DRSAR-RDF, SYS DEV DIV - FUZES
ATTN DRSAR-ASF, FUZE AND MUNITIONS
SUPPORT DIV
ROCK ISLAND, IL 61201

US ARMY ELECTRONICS TECHNOLOGY
& DEVICES LABORATORY
ATTN DELET-DD
FT MONMOUTH, NJ 07703

HQ, USAF/SAMI
WASHINGTON, DC 20330

DIRECTOR
DEFENSE ADVANCED RESEARCH
PROJECTS AGENCY
ARCHITECT BLDG
ATTN DIR, NUCLEAR MONITORING
RES OFFICE
1400 WILSON BLVD
ARLINGTON, VA 22209

DEFENSE COMMUNICATIONS
ENGINEERING CENTER
ATTN TECHNICAL LIBRARY
1860 WIEHLE AVE
RESTON, VA 22090

DIRECTOR
DEFENSE COMMUNICATIONS AGENCY
ATTN TECH LIBRARY
WASHINGTON, DC 20305

DIRECTOR
DEFENSE COMMUNICATIONS AGENCY
NATIONAL MILITARY COMMAND
SYSTEM SUPPORT CENTER
ATTN TECHNICAL DIRECTOR (B102)
WASHINGTON, DC 20301

DIRECTOR
DEFENSE NUCLEAR AGENCY
ATTN RAEV, ELECTRONICS VULNERABILITY DIV
ATTN TITL, TECHNICAL LIBRARY DIV
ATTN TISI, SCIENTIFIC INFORMATION DIV
WASHINGTON, DC 20305

UNDER SECRETARY OF DEFENSE FOR
RESEARCH & ENGINEERING
ATTN ASST DIR (ELECTRONICS & PHYSICAL
SCIENCES)
ATTN ASST DIR (ENG TECHNOLOGY)
ATTN DEP DIR (STRATEGIC & SPACE SYS)
WASHINGTON, DC 20301

COMMANDER
FIELD COMMAND
DEFENSE NUCLEAR AGENCY
ATTN FCSD-A4, TECH REF BR
KIRTLAND AFB, NM 87115

DIRECTOR
NATIONAL SECURITY AGENCY
ATTN TECHNICAL LIBRARY
FT MEADE, MD 20755

OFFICE, DEPUTY CHIEF OF STAFF
FOR OPERATIONS & PLANS
DEPT OF THE ARMY
ATTN DAMO-SSA, NUCLEAR/CHEMICAL
PLANS & POLICY DIV
WASHINGTON, DC 20310

COMMANDER
US ARMY COMMUNICATIONS COMMAND
ATTN TECH LIB
FT HUACHUCA, AZ 85613

CHIEF
US ARMY COMMUNICATIONS SYS AGENCY
ATTN SCCM-AD-SV, LIBRARY
FT MONMOUTH, NJ 07703

DISTRIBUTION (Cont'd)

COMMANDER
US ARMY NUCLEAR & CHEMICAL AGENCY
ATTN TECH LIB
BUILDING 2073
7500 BACKLICK ROAD
SPRINGFIELD, VA 22150

COMMANDER
CORPS OF ENGINEERS
HUNTSVILLE DIVISION
PO BOX 1600
ATTN T. BOLT
HUNTSVILLE, AL 35807

COMMANDER
NAVAL SURFACE WEAPONS CENTER
ATTN F-30, NUCLEAR EFFECTS DIV
WHITE OAK, MD 20910

COMMANDER
AF WEAPONS LAB, AFSC
ATTN SE, NUCLEAR SYS DIV
ATTN EL, ELECTRONICS DIV
KIRTLAND AFB, NM 87117

LAWRENCE LIVERMORE NATIONAL LABORATORY
PO BOX 808
ATTN E. K. MILLER
LIVERMORE, CA 94550

LAWRENCE LIVERMORE NATIONAL LABORATORY
PO BOX 5504, L-156
ATTN H. CABAYAN
LIVERMORE, CA 94550

ELECTROMAGNETIC APPLICATIONS, INC
ATTN R. A. PERALA
1990 S. GARRISON STREET
DENVER, CO 80226

ITT RESEARCH INSTITUTE
ATTN I. N. MINDEL
ATTN J. E. BRIDGES
10 W. 35TH STREET
CHICAGO, IL 60616

KAMAN SCIENCES CORP
PO BOX 7463
ATTN TECH LIBRARY
COLORADO SPRINGS, CO 80933

PATRIOT MISSILE SYSTEM
USADARCOM
ATTN PROJECT MANAGER'S OFFICE
MR. W. NEWBY
REDSTONE ARSENAL, AL 35809

STANFORD RESEARCH INSTITUTE
3980 EL CAMINO REAL
ATTN A. L. WHITSON
PALO ALTO, CA 94306

US ARMY ELECTRONICS RESEARCH
& DEVELOPMENT COMMAND
ATTN TECHNICAL DIRECTOR, DRDEL-CT

HARRY DIAMOND LABORATORIES
ATTN CO/TD/TSO/DIVISION DIRECTORS
ATTN RECORD COPY, 81200
ATTN HDL LIBRARY, 81100 (2 COPIES)
ATTN HDL LIBRARY, 81100 (WOODBIDGE)
ATTN TECHNICAL REPORTS BRANCH, 81300
ATTN CHAIRMAN, EDITORIAL COMMITTEE
ATTN LEGAL OFFICE, 97000
ATTN CHIEF, 21000
ATTN CHIEF, 21100
ATTN CHIEF, 21200
ATTN CHIEF, 21300
ATTN CHIEF, 21400 (4 COPIES)
ATTN CHIEF, 21500
ATTN CHIEF, 22000
ATTN CHIEF, 22100
ATTN CHIEF, 22300
ATTN CHIEF, 22800
ATTN CHIEF, 22900
ATTN CHIEF, 20240 (2 COPIES)
ATTN MORRISON, R. E., 13500 (GIDEP)
ATTN INGERSOLL, P., 34300
ATTN CHASE, R., 21100
ATTN MEYER, O. L., 22300
ATTN SCOTT, W. J., 21500
ATTN REYZER, R., 21300
ATTN FEMENIAS, R., 21100
ATTN LOFTUS, J. J., 21400
ATTN CUNEO, A. A., 21400 (30 COPIES)

DATE
FILMED
— 8